Journal of Inorganic Biochemistry 197 (2019) 110695

Contents lists available at ScienceDirect

Journal of Inorganic Biochemistry

journal homepage: www.elsevier.com/locate/jinorgbio

Focused review

Azaindoles: Suitable ligands of cytotoxic transition metal complexes

Pavel Štarha*, Zdeněk Trávníček

Biologically Active Complexes and Molecular Magnets, Regional Centre of Advanced Technologies and Materials, Faculty of Science, Palacký University in Olomouc, Šlechtitelů 27, 783 71 Olomouc, Czech Republic

ARTICLE INFO

Keywords:
Azaindole
Complexes
Cytotoxicity
Anticancer activity

ABSTRACT

This minireview is devoted to the complexes of various transition metals, which contain azaindole ring coordinated to the metal centre, and whose cytotoxicity was studied. We decided to overview this interesting group of coordination compounds with the aim to highlight various structural types of complexes depending on the metal centre (*i.e.*, Pt, Pd, Ru, Ir or Au) and type of the used co-ligand(s). The presented complexes are also reviewed in context of their toxicity, selectivity and processes connected with their mechanism of action. Some of complexes were also studied on *in vivo* models showing promising results comparable with the commonly used anticancer drug *cisplatin*. It can be deduced from the herein overviewed literature data regarding transition metal complexes containing azaindoles as ligands, that at least a few of them may represent suitable and promising candidates in the field of anticancer therapy. As one of the examples, the *cis*-[PtI_2(*2Me4Cl*-7aza)$_2$] complex (*2Me4Cl*-7aza = 2-methyl-4-chloro-7-azaindole) should be mentioned, which showed considerably higher *in vitro* cytotoxicity than *cisplatin*, the ability to overcome both the acquired and natural resistance of human cancer cells in comparison with the biological action of *cisplatin*, different mechanism of action than *cisplatin* and comparable *in vivo* anticancer activity with *cisplatin*.

1. Introduction

A family of azaindoles involves four isomers, namely 4-azaindole (1*H*-pyrrolo[3,2-*b*]pyridine; 4aza), 5-azaindole (1*H*-pyrrolo[3,2-*c*]pyridine; 5aza), 6-azaindole (1*H*-pyrrolo[2,3-*c*]pyridine; 6aza) and 7-azaindole (1*H*-pyrrolo[2,3-*b*]pyridine; 7aza), according the mutual position of the nitrogen atoms of the fused pyridine and pyrrole rings (Fig. 1). All these isomers represent suitable scaffolds for a number of derivatives showing various types of biological activities [1], such as p21-activated kinase-1 (PAK1) inhibition [2], cell division cycle 7 (Cdc7) kinase inhibition [3] or cytotoxicity mediated through the tubulin polymerization inhibition [4]. Concerning the transition metal complexes, the complexes containing 4aza-, 5aza- or 6aza-based ligands are quite rare in the literature [5,6]. On the other hand, numerous complexes containing 7aza-based ligands have been reported by several research groups [7–15]. Their applicability seems to be quite extensive, since several research groups reported 7aza-containing luminescent materials for *e.g.*, chemical sensors/probes or bioimaging [7], or 7aza-containing complexes exhibiting relevant biological activity (*e.g.*, cytotoxicity). The later agents are overviewed in this focused review, because our group contributed substantively to this area in last couple of years.

Concerning the coordination chemistry of 7aza within the structures of transition metal complexes, various coordination modes have been reported to date (Fig. 2). In particular, 7aza acts mainly as a monodentate *N*-donor ligand coordinated through either *N*7 [14] or deprotonated *N*1 [15] nitrogen atom. Expectably, 7aza forms a number of multinuclear (especially dinuclear) complexes, where it connects the metal centres as the *N1*,*N7*- [16], *C2*,*N7*- [17], *C6*,*N7*- [16] and even *N1*,*N1*,*N7*-bridging ligand [16]. The *C2*-coordination was observed for the [Pt(CH_3)(MeCN)(*py*-7aza$^-$)] complex (CSD refcode HEYYEQ) containing 1-(pyridin-2-yl)-7-azaindole (*py*-7aza) acting as the chelating $C2^{aza}$,N^{py}-donor ligand [17].

As for the content of this review we focused only on the transition metal complexes of azaindoles for which, to the best of our knowledge, the cytotoxicity has been studied. In this review, we decided to start with the platinum complexes, because the most representatives of biologically active transition metal complexes containing azaindoles have been reported for this metal. After that we overviewed markedly less numerous examples of ruthenium, palladium, iridium and gold complexes containing the 7aza-based ligand(s), whose biological activity has been described as well, and these complexes are ordered according the proton number of the respective metal. Besides complexes bearing the 7aza-based ligands, the highly cytotoxic platinum(II)

* Corresponding author.
E-mail address: pavel.starha@upol.cz (P. Štarha).

https://doi.org/10.1016/j.jinorgbio.2019.110695
Received 15 February 2019; Received in revised form 10 April 2019; Accepted 21 April 2019
Available online 24 April 2019
0162-0134/

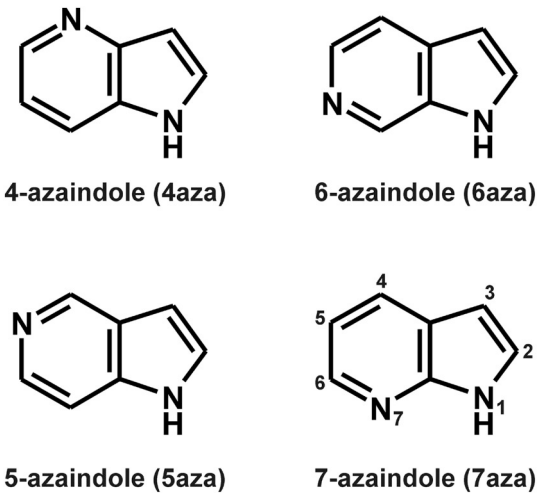

Fig. 1. Structural formulas of all four azaindole isomers, given together with the atom numbering scheme (for 7aza).

diiodido complexes containing 4-azaindole-based ligand(s) [18] or complex *cis*-[Ru(*n*aza)(bpy)$_2$Cl]$^+$ (*n*aza = 4aza or 5aza; bpy = 2,2′-bipyridine) [5] represent the first biologically studied complexes with different azaindole than 7aza. Further it has to be stated that no bioanalysed transition metal complexes containing 6aza-based ligands were reported to date. In this context, complexes containing 9*H*-*β*-carboline (norharmane) can be mentioned, because norharmane involves 6aza ring in its structure [19]. However, we did not include these complexes and complexes containing similar ligands (*e.g.*, *α*-carboline or γ-carboline) to this review, because they are structurally different (three fused rings) from azaindoles themselves (two fused rings).

2. Platinum(II) complexes

Platinum complexes are widely studied for their anticancer activity, following the clinical success of *cisplatin* and analogues [20,21]. Among the pharmacologically prospective *cisplatin*-derived complexes, numerous examples are based on diverse heterocyclic ligands. For example, *picoplatin* has entered (but not passed) the clinical trials on human oncological patients [22], and complexes containing various 1,10-phenanthroline derivatives showed extremely high, submicromolar *in vitro* cytotoxicity against various human cancer cell lines [23]. That is why the utilization of heterocyclic ligands for the development of new biologically prospective platinum complexes has to be accepted as reasonable and, as supported by the literature data and the following text, provably leading to relevant outputs.

2.1. Dichlorido complexes

2.1.1. Complexes of the *cis*-[Pt(n7aza)$_2$Cl$_2$] type

Harrison et al. reported the *cisplatin*-derived complex *cis*-[Pt(7aza)$_2$Cl$_2$] in 1984, which was markedly more toxic (LD$_{50}$ = 110 mg/kg) in the treated rats than its diiodido and oxalato analogues (see below) with, while this complex showed low anticancer effect (*i.e.*, below the level considered as significant) at various models (*e.g.*, against P388 lymphocytic leukaemia at doses up to 400 mg/kg) in rats; LD$_{50}$ = amount of a substance required to kill half of the tested animals [8].

In 2012, we followed the work of Harrison et al. [8] and revisited the cytotoxicity studies of complex *cis*-[Pt(7aza)$_2$Cl$_2$] [9]. It was of great interest to investigate whether this complex affects the viability of the treated cancer cells *in vitro*, similarly as observed couple of years earlier by Hambley's group for moderately cytotoxic ammine complexes *cis*-[Pt(7aza)Cl$_2$(NH$_3$)] and *trans*-[Pt(7aza)Cl$_2$(NH$_3$)] (see Section 2.1.2) [10].

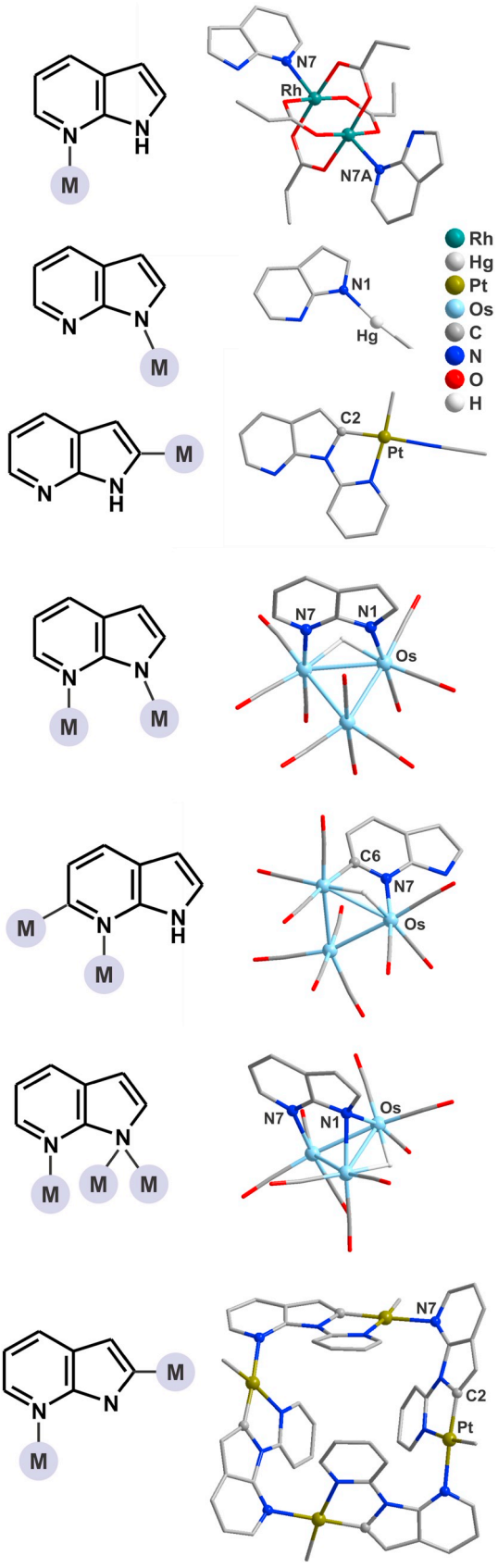

(caption on next page)

Fig. 2. Coordination modes of the 7-azaindole (7aza) moiety reported to date for the crystallographically determined molecular structures of the transition metal complexes containing the 7aza-based ligands. Molecular structures of $[Rh_2(\mu\text{-pac})_4(7aza)_2]$ (N7 in the drawing = N1 in the CIF file; N7A = N3), [Hg(7aza$^-$)(CH_3)], [Pt(CH_3)(MeCN)(*py*-7aza)] (C2 = C1), $[Os_3(\mu\text{-}7aza^-)(\mu\text{-H})(CO)_{10}]$ (N7 = N1; N1 = N2), $[Os_3(\mu\text{-}7aza^-)(\mu\text{-H})(CO)_9]$ (N7 = N1; N1 = N2), $[Os_3(\mu\text{-}7aza^-)(\mu\text{-H})(CO)_{10}]$ (N7 = N1; C6 = C11) and $[Pt_4(\mu\text{-}py\text{-}7aza)_4(CH_3)_4]\cdot 2bz$ (N7 = N11). Hydrogen atoms (except the hydrido ligands) and bz molecules of crystallization were omitted for clarity. Different labels than in deposited CIF files were used in some cases, as specified in parentheses. Hpac = propanoic acid; *py*-7aza = 1-(pyridin-2-yl)-7-azaindole, bz = benzene. Structural data were published in [14–17] (CSD refcodes (from top to bottom): PRNRHB, JESPEC, HEYYEG, RONBAX, RONBEB, RONBIF, and HEYYIU, respectively).

These complexes are formally derived from *cisplatin* by the replacement of one ammine ligand by one 7aza molecule, while the replacement of both NH_3 ligands in the structure of *cisplatin* provides the mentioned complex *cis*-$[Pt(7aza)_2Cl_2]$. Further motivations for the investigation of complex *cis*-$[Pt(7aza)_2Cl_2]$ were based on the possibilities of utilization of various 7aza derivatives including various highly biologically active ones [24,25]. Last but not least, it is known, for example, for some platinum(II) diiodido complexes, such as *cis*-$[PtI_2(NH_3)_2]$ or [Pt(dach)I_2], that they showed significant cytotoxicity against cancer cell lines in the *in vitro* level despite they were reported as anticancer inactive *in vivo*; dach = cyclohexane-1,2-diamine [26]. However, the solubility of complex *cis*-$[Pt(7aza)_2Cl_2]$ showed to be very low under the experimental conditions used for the biological testing (solubility $\leq$1.0 μM), preventing the relevant investigation of its *in vitro* cytotoxicity at the representative human cancer cells (IC_{50} $^{>}$1.0 μM at the HOS osteosarcoma and MCF-7 breast adenocarcinoma cells; IC_{50} = half maximal inhibitory concentration).

In order to improve the solubility of dichloridoplatinum(II) complexes with 7aza-based ligands, various halogeno *C*-derivatives of 7aza were used [27–30] instead of the parent unsubstituted 7aza [8,9]. Complexes were synthesized by a stoichiometric reaction of $K_2[PtCl_4]$ with the appropriate *n*7aza compound in water/ethanol mixture (1:1, v/v) for 24–48 h at 50 °C; *n*7aza = 3-chloro-7-azaindole (*3Cl*-7aza), 3-bromo-7-azaindole (*3Br*-7aza), 3-iodo-7-azaindole (*3I*-7aza), 4-chloro-7-azaindole (*4Cl*-7aza), 4-bromo-7-azaindole (*4Br*-7aza for complex **1**), 5-bromo-7-azaindole (*5Br*-7aza for complex **2**), 3-chloro-5-bromo-7-azaindole (*3Cl5Br*-7aza) and 3-iodo-5-bromo-7-azaindole (*3I5Br*-7aza) (Fig. 3). Indeed, the improved solubility of *cis*-$[Pt(n7aza)_2Cl_2]$ complexes allowed the *in vitro* cytotoxicity testing at the pharmacologically relevant scale up to the 50 μM concentration. Among these complexes, several representatives showed even > 10-fold higher cytotoxic activity than the used reference drug *cisplatin* at various human cancer cell lines, including the cells with intrinsic (*e.g.*, HOS) or acquired (A2780R *cisplatin*-resistant ovarian carcinoma) resistance to *cisplatin* (Table 1). Dichlorido *cis*-$[Pt(n7aza)_2Cl_2]$ complexes also showed an ability to overcome the acquired resistance of human cancer cells towards *cisplatin*, because their Resistance Factor (RF) equalled 0.7–1.2 at the *in vitro* A2780/A2780R model (A2780 = human ovarian carcinoma cell line); RF = IC_{50}(resistant cells)/IC_{50}(sensitive cells).

Complex **1** was highly hydrolytically stable in the used DMF-d_7/D_2O mixture (1:1, *v/v*) and readily interacted (*ca.* 50% of the starting complex **1** after 48 h of standing at ambient temperature) with the naturally-occurring reduced glutathione (GSH) [29]. Bearing in mind that glutathione is generally accepted as being responsible for a deactivation of various xenobiotics (including metal-based drugs), making this intracellular thiol a crucial factor of the cancer cell resistance, we co-studied the less effective complex *cis*-$[Pt(3Cl5Br\text{-}7aza)_2Cl_2]$ with complex **1**. Indeed, the complex *cis*-$[Pt(3Cl5Br\text{-}7aza)_2Cl_2]$ interacted with GSH more rapidly than **1**, because no signs of the parent complex *cis*-$[Pt(3Cl5Br\text{-}7aza)_2Cl_2]$ were detected in the ^{1}H NMR spectra after 48 h of standing at ambient temperature.

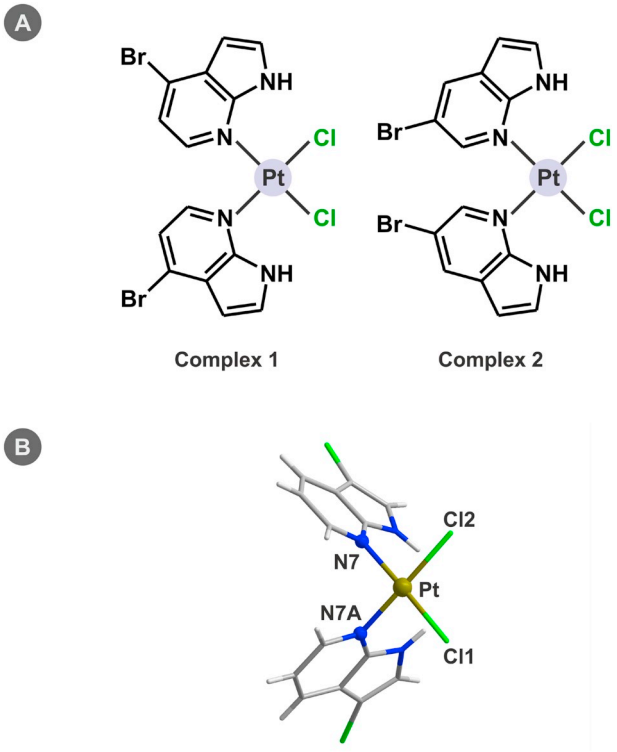

Fig. 3. Structural formulas of *cis*-$[Pt(4Br\text{-}7aza)_2Cl_2]$ (**1**) and *cis*-$[Pt(5Br\text{-}7aza)_2Cl_2]$ (**2**) (**A**; *4Br*-7aza = 4-bromo-7-azaindole, *5Br*-7aza = 5-bromo-7-azaindole), and the molecular structure of *cis*-$[Pt(3Cl\text{-}7aza)_2Cl_2]\cdot$DMF (DMF molecule of crystallization was omitted for clarity). Structural data were published in [27] (CSD refcode: YEFJAW) (**B**; *3Cl*-7aza = 3-chloro-7-azaindole).

In order to shed light on the mechanism of action of *cis*-$[Pt(n7aza)_2Cl_2]$ complexes, various processes were studied and reported [27,30]. Complexes *cis*-$[Pt(n7aza)_2Cl_2]$ terminated the RNA synthesis (T7 RNA polymerase at the 212-bp fragment of the pSP73KB plasmid DNA) as a consequence of the covalent binding of these agents to the used DNA template; *n*7aza = *3Cl*-7aza, *3I*-7aza and *5Br*-7aza [27]. The sequence analysis proved that the *cis*-$[Pt(n7aza)_2Cl_2]$ complexes bind DNA similarly (*i.e.*, form similar DNA adducts) as conventional *cisplatin* (preferentially at GG and AG sites). Further, *cis*-$[Pt(3Cl\text{-}7aza)_2Cl_2]$ and *cis*-$[Pt(3I\text{-}7aza)_2Cl_2]$ were accumulated (*e.g.*, 3732 pmol Pt/10^6 cells for *cis*-$[Pt(3Cl\text{-}7aza)_2Cl_2]$) and platinated DNA (*e.g.*, 4.7 pmol Pt/μg DNA for *cis*-$[Pt(3Cl\text{-}7aza)_2Cl_2]$) at the treated A2780 cells much better than *cisplatin* (83 pmol Pt/10^6 cells; 0.3 pmol Pt/μg DNA) [30]. In connection with the above discussed results of transcription mapping of DNA adducts [27], these experiments proved DNA as a potential intracellular target (but not necessarily the only one) of *cis*-$[Pt(n7aza)_2Cl_2]$ complexes [30]. The determination of monofunctional adducts and interstrand cross-linking efficiency (cell-free DNA binding experiments) proved the formation of similar DNA adducts of *cis*-$[Pt(n7aza)_2Cl_2]$ complexes and *cisplatin* [30]. However, it has to be taken into account that although *cis*-$[Pt(n7aza)_2Cl_2]$ complexes and *cisplatin* form the same covalent adducts with DNA, *cis*-$[Pt(n7aza)_2Cl_2]$ complexes possibly induce different DNA conformation changes than *cisplatin* thanks to the bulkier *N*-donor ligand (*i.e.*, *n*7aza) in their structures. It is known that a different distortion of the DNA conformation affects differently various intracellular processes. Indeed, *cis*-$[Pt(n7aza)_2Cl_2]$ complexes induced different cell cycle modification (high sub-G_1 population) than *cisplatin* (G_2/M arrest) at the A2780 cells. In other words, the DNA synthesis inhibition induced by similar DNA adducts with *cis*-$[Pt(n7aza)_2Cl_2]$ complexes or *cisplatin* is markedly more lethal to the cells treated by *cis*-$[Pt(n7aza)_2Cl_2]$ complexes than for *cisplatin*.

Also of importance, the adducts of *cis*-$[Pt(n7aza)_2Cl_2]$ complexes

Table 1
The selected *in vitro* cytotoxicity results reported for the best-performing compounds of all the overviewed types of complexes containing azaindole-based ligands. Relative Activity (RA) = IC_{50}(*cisplatin*)/IC_{50}(complex) and Resistance Factors (RF) = IC_{50}(resistant cells)/IC_{50}(sensitive cells) obtained for the overviewed complexes using the A2780 (human ovarian carcinoma cell line) and its *cisplatin*-resistant variant (A2780R). All the complexes were pre-dissolved in DMF, except for complexes **18–21** tested in the presence of DMSO.

Complex	Cell lines	Cytotoxicity (IC_{50}; μM)	RA	RF	Ref.
cis-[Pt(*4Br*-7aza)$_2$Cl$_2$] (**1**)	A2780, A2780R, HOS, G-361, MCF-7, A549, HeLa, LNCaP	3.8, 3.5, 4.5, 2.7, 2.7, 11.1, 9.2, 4.0	5.7, 9.1, 5.6, 2.1, 6.7, > 4.5, 4.3, 1.0	0.9	[29]
cis-[Pt(*5Br*-7aza)$_2$Cl$_2$] (**2**)	A2780, A2780R, HOS, G-361, MCF-7, A549, HeLa, LNCaP	1.8, 2.1, 2.5, 0.6, 2.0, 4.9, 4.3, 1.5	6.7, 12.8, 13.7, 5.7, 9.8, 5.3, 2.3, 2.5	1.2	[29]
cis-[Pt(7aza)Cl$_2$(NH$_3$)] (**3**)	A2780	3.6	0.4		[10]
trans-[Pt(7aza)Cl$_2$(NH$_3$)] (**4**)	A2780	6.0	0.2		[10]
cis-[Pt(*1Me*-7aza)Cl$_2$(NH$_3$)] (**5**)	A2780, A2780R, MCF-7, HCT116$^+$, HCT116$^-$	4.2, 4.3, 14.0, 10.2, 15.0	0.6, 3.6, 2.1, 0.6, 0.9	1.0	[11]
trans-[Pt(*1Me*-7aza)Cl$_2$(NH$_3$)] (**6**)	A2780, A2780R, MCF-7, HCT116$^+$, HCT116$^-$	3.6, 2.8, 12.0, 5.2, 6.4	0.7, 5.6, 2.5, 1.1, 2.2	0.8	[11]
cis-[Pt(*4Br*-7aza)$_2$I$_2$] (**7**)	A2780, A2780R, HOS, G-361, MCF-7, A549, HeLa, 22Rv1, Caco-2	3.2, 3.3, 0.4, 3.2, 1.0, 4.3, 3.8, 3.8, 0.4	8.8, > 15.2, 47.3, 1.7, 17.9, > 11.6, 8.0, 7.1, > 225.0	1.0	[33]
cis-[PtI$_2$(*2Me4Cl*-7aza)$_2$] (**8**)	A2780, A2780R, HOS, G-361, MCF-7, A549, HeLa, 22Rv1, Caco-2	1.7, 1.0, 0.7, 1.7, 2.1, 3.5, 3.8, 3.5, 0.4	16.5, > 50.0, 27.0, 3.1, 8.5, > 14.3, 8.0, 7.7, > 225.0	0.6	[33]
cis-[Pt(*ip*-4aza)$_2$I$_2$] (**9**)	A2780, A2780R, HT-29	3.8, 2.9, 4.9	7.0, > 17.2, > 10.2	0.8	[18]
cis-[Pt(*ip*-4aza)I$_2$(NH$_3$)] (**10**)	A2780, A2780R, HT-29	8.9, 12.1, 8.0	3.0, > 4.1, > 6.3	1.4	[18]
[Pt(*3Br*-7aza)$_2$(ox)] (**11**)	A2780, A2780R, HOS, G-361, MCF-7, A549, HeLa	19.2, > 50.0, 27.5, 17.3, 18.3, > 50.0, 31.8	1.1, < 0.6, 0.9, 0.3, 1.0, -, 1.3, < 0.1	> 2.6	[34]
[Pt(*4Br*-7aza)$_2$(cbdc)] (**12**)	A2780, LNCaP, PC-3	5.1, 23.5, 26.6	4.3, > 2.1, > 1.9		[35]
[Pt(*5Br*-7aza)$_2$(cbdc)] (**13**)	A2780, LNCaP, PC-3	4.7, 22.1, 29.6	4.6, > 2.3, < 1.7		[35]
[Pt(*3I*-7aza)$_2$(mal)] (**14**)	A2780, A2780R	26.6, 28.9	1.0, > 1.7	1.1	[36]
[Pt(*4Br*-7aza)$_2$(mal)] (**15**)	A2780, A2780R	24.4, 22.8	1.1, > 2.2	0.9	[36]
cis-[Pt(*3Br*-7aza)$_2$(dec)$_2$] (**16**)	A2780, A2780R	14.5, 14.5	1.8, > 3.4	1.0	[36]
cis-[Pt(*4Br*-7aza)$_2$(dec)$_2$] (**17**)	A2780, A2780R	14.1, 19.5	1.9, > 2.6	1.4	[36]
[Pt(dmba$^-$)(7aza$^-$)(dmso)] (**18**)	T47D, A2780, A2780R	0.5, 0.3, 0.5	69.8, 2.6, 24.4	1.7	[12]
[Pt(7aza^1)Cl(dmba$^-$)] (**19**)	T47D, A2780, A2780R	13.0, 7.0, 7.6	2.5, 0.2, 1.7	1.1	[37]
trans-[Pd(*3Ca*-7aza)$_2$Cl$_2$] (**20**)	T47D, MCF-7, A549, A2780	4.8, 6.0, 6.1, 3.7	3.4, 1.1, 0.5, 0.4		[58]
trans-[Pd(*4Br*-7aza)$_2$Cl$_2$] (**21**)	T47D, MCF-7, A549, A2780	59.1, 42.3, 46.9, 30.3	0.3, 0.2, 0.1, 0.1		[59]
[Ir(η^5-Cp^{ph})(*py*-7aza)Cl]PF$_6$ (**22**)	A2780, A2780R, HCT116, HeLa, MCF-7, DU-145, A549	3.1, 17.4, 10.4, 10.5, 6.9, 13.0, 9.1	2.3, 1.2, 2.2, 1.1, 3.1, 0.4, 0.7	5.6	[63]
[Ir(η^5-Cp^{ph})(*py*-7aza)Cl]PF$_6$ (**23**)	A2780, A2780R	20.2, > 25.0	0.4, < 0.8	> 1.2	[63]
[Au(*5Br*-7aza)(PPh$_3$)] (**24**)	A2780, A2780R	3.1, 14.4	6.5, > 3.5	4.6	[67]
[Au(*2Me4Cl*-7aza)(PPh$_3$)] (**25**)	A2780, A2780R	2.8, 8.9	7.3, > 5.6	3.2	[67]

with DNA were more resistant to the nucleotide excision repair than observed for *cisplatin*–DNA adducts, which correlates with low RF of *cis*-[Pt(*n*7aza)$_2$Cl$_2$] complexes at the A2780/A2780R model (*vide supra*). It was also proved that *cis*-[Pt(*n*7aza)$_2$Cl$_2$] complexes induce apoptosis more effectively than *cisplatin*. The discussed differences at various aspects connected with the mechanism of action are suggestive for different molecular mechanism of action arising from the replacement of both ammines of *cisplatin* by the bulkier *n*7aza ligands in *cis*-[Pt(*n*7aza)$_2$Cl$_2$] complexes.

The *in vitro* studies were followed by *in vivo* anticancer activity studies for complexes *cis*-[Pt(*n*7aza)$_2$Cl$_2$] (*n*7aza = *3Cl*-7aza, *3I*-7aza and *5Br*-7aza) [28]. These complexes did not reduce the tumour tissue as effectively (8% decrease of tumour tissue weight for *cis*-[Pt(*5Br*-7aza)$_2$Cl$_2$]) as *cisplatin* (50% decrease of tumour tissue weight); 7-day dosing schedule (3 mg/kg). On the other hand, *cis*-[Pt(*n*7aza)$_2$Cl$_2$] complexes induced less serious side effects in the treated animals as compared with *cisplatin*-treated mice, for which *e.g.*, loss of weight, fatigue and loss of appetite were observed. Following *ex vivo* studies proved that complex *cis*-[Pt(*5Br*-7aza)$_2$Cl$_2$], the best-performing one in the *in vitro* level of testing, effectively modulated the level of initiator caspase 8, effector caspase 3 and regulatory protein p53, indicating that the apoptotic cancer cell death is induced through the intrinsic (mitochondrial) pathway.

2.1.2. Complexes of the [Pt(n7aza)Cl$_2$(NH$_3$)] type

Complex *cis*-[Pt(7aza)Cl$_2$(NH$_3$)] (**3**) was prepared from (NH$_4$)[PtCl$_3$(NH$_3$)] interacting with an equimolar amount of 7aza in acidified water/ethanol mixture (5 days of stirring in the dark), and complex *trans*-[Pt(7aza)Cl$_2$(NH$_3$)] (**4**) formed when *cisplatin*, 7aza and AgNO$_3$ were allowed to interact, and the formed *cis*-[Pt(7aza)$_2$(NH$_3$)$_2$]$^{2+}$ intermediate reacted with HCl (Fig. 4) [10]. Complexes **3** and **4** were less *in vitro* cytotoxic against the A2780 cells than *cisplatin* (Table 1). A fluorescent 7aza ligand was used in order to study the metabolism of cytotoxic Pt(II) complexes in the treated cancer cells. A fluorescence of 7aza completely quenched with its coordination to the central Pt(II) atom, but it was observed again when complex **3** was mixed with the sulfur-containing biomolecule cysteine (CySH; *e.g.*, 20% of the intensity of free 7aza after 7 days), GSH or methionine, which was not a case of *trans*-isomer **4**. On the other hand, the fluorescence implied the gradual release of 7aza from the structure of both complexes **3** and **4** at the treated A2780 cells (following the two-photon excitation).

Similar complexes, namely *cis*-[Pt(*1Me*-7aza)Cl$_2$(NH$_3$)] (**5**) and *trans*-[Pt(*1Me*-7aza)Cl$_2$(NH$_3$)] (**6**), contain the *N*1-alkylated derivative 1-methyl-7-azaindole (*1Me*-7aza; Fig. 4) [11,31,32]. Complex **5**, similarly to **3**, was prepared by the direct reaction of K[PtCl$_3$(NH$_3$)] (instead of the ammonium salt used in the case of **3**) with *1Me*-7aza (methanol, slight excess of *1Me*-7aza, stirred at room temperature for 4 days). On the other hand, complex **6** was synthesized using a different procedure than used for the structurally similar complex **4**. In particular, the key intermediate *cis*-[Pt(*1Me*-7aza)$_2$(NH$_3$)$_2$]$^{2+}$ was prepared from *cis*-[PtI$_2$(NH$_3$)$_2$] after its dehalogenation (by AgNO$_3$) and reaction with an excess of *1Me*-7aza. KI was added to the solution of the obtained complex *cis*-[Pt(*1Me*-7aza)$_2$(NH$_3$)$_2$]$^{2+}$ providing the iodido complex *trans*-[PtI$_2$(*1Me*-7aza)(NH$_3$)] after the silica gel chromatography. Complex *trans*-[PtI$_2$(*1Me*-7aza)(NH$_3$)] was dehalogenated (again by silver nitrate) and KCl was poured in to get the final complex **6** (again after the silica gel chromatography). Both complexes **5** and **6** exceeded the *in vitro* cytotoxicity of *cisplatin* at the MCF-7 and A2780R cells, but not at the A2780 cells (Table 1) [11]. The Selectivity index (SI; defined as the ratio of IC_{50}(healthy cells)/IC_{50}(cancer cells)) equal 3.4–12.1 for **5** and 1.4–6.1 for **6** at the used human cancer cells (2.3–28.8 for *cisplatin*). Both complexes **5** and **6** (RF = 1.0 and 0.8, respectively; A2780/A2780R model) overcome the resistance of the cancer cells against *cisplatin* (RF = 6.5).

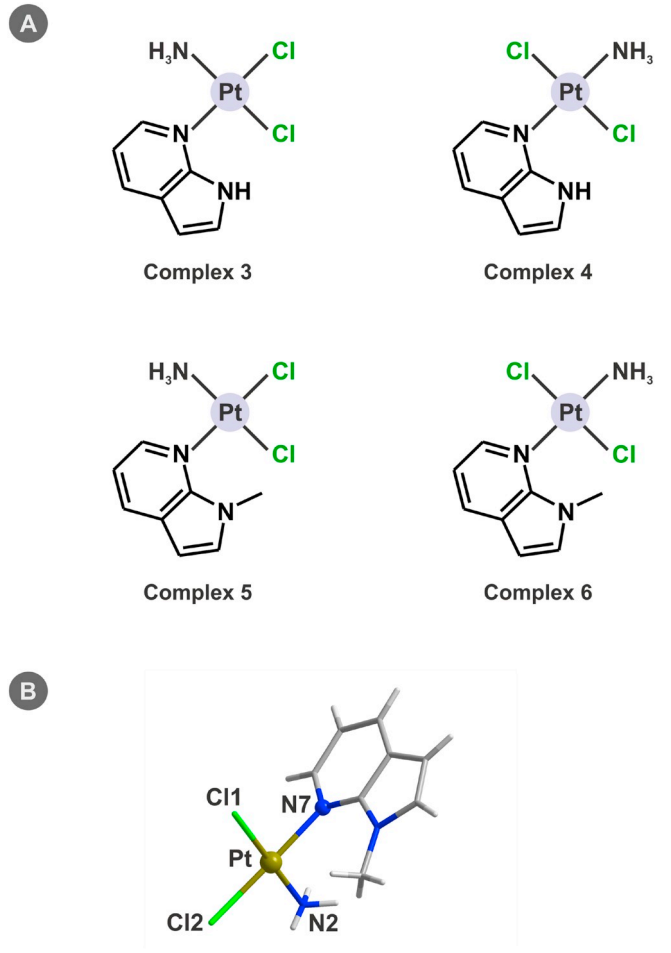

Fig. 4. Structural formulas of *cis*-[Pt(7aza)Cl_2(NH_3)] (**3**), *trans*-[Pt(7aza)Cl_2(NH_3)] (**4**), *cis*-[Pt(*1Me*-7aza)Cl_2(NH_3)] (**5**) and *trans*-[Pt(*1Me*-7aza)Cl_2(NH_3)] (**6**) (**A**; 7aza = 7-azaindole, *1Me*-7aza = 1-methyl-7-azaindole), and the molecular structure of **5**. Structural data were published in [11] (CSD refcode BUFQEA) (**B**).

In general, different RF values usually point out a different mechanism of action, in this case for complexes **5** and **6** as compared with *cisplatin*. The authors proved that an ability of **5** to overcome the acquired resistance of the A2780 cells to *cisplatin* is not connected with its enhanced accumulation. At first, complex **5** (RF = 1.0) had similar level of Pt accumulated by both the A2780 and A2780R cells, secondly, complex **5** was markedly more potent at the A2780R cells than *cisplatin* (RA = 3.6), although both agents were accumulated at the same level after 24 h exposure (126 and 128 pmol Pt/10^6 cells for **5** and *cisplatin*, respectively). On the other hand, the cellular uptake of the *trans*-complex **6** was considerably higher than for *cisplatin* at the A2780 and A2780R cells. Higher accumulation of **6** at the treated cancer cells than for **5** correlates with lower lipophilicity of the latter complex (log*P* = −0.66, and 0.83, respectively). Further, in contrast to rapidly accumulated complexes of the *cis*-[Pt(*n*7aza)$_2$$Cl_2$] type (*vide supra*), the cell uptake of complexes **5** and **6** is not as much higher as compared to *cisplatin*.

Complexes **5** and **6** platinated the nuclear DNA of the A2780, A2780R and MCF-7 cells in higher extent than *cisplatin*, but any relationship between the DNA platination and intracellular accumulation was not derived from the obtained results. However, the obtained results proved that low cytotoxicity of *cisplatin* at the A2780R cells does not result only from the reduced cellular uptake (see above), but it is also connected with higher rate of DNA repair, which was not proved for **5** and **6**.

Complex **6** exhibited higher affinity towards DNA and the model intracellular protein (human serum albumin; HSA) than **5**, and the latter observation (affinity towards intracellular proteins) could be understood as the explanation of different activity of both complexes. A transcription mapping of DNA adducts of complexes **5** and **6** was performed with the T7 RNA polymerase at the 212-bp fragment of the pSP73KB plasmid DNA. Similarly as described above for the *cis*-arranged *cis*-[Pt(*n*7aza)$_2$$Cl_2$] complexes [27], the DNA binding modes for complex **5** was analogical to *cisplatin*, but in the case of complex **6** it was distinct from *cisplatin* but similar to another used reference complex, *transplatin* [11]. The confocal microscopy visualization of the treated A2780 cells showed that the subcellular localization of complexes **5** and **6** is more or less non-nuclear (*e.g.*, lysosomes or late endosomes). Complex **5** and *cisplatin* induced the same cell cycle modification of the treated A2780 cells (high sub-G_1 and G_2/M populations), implying the same mechanism of action of both agents, while the *trans*-complex **6** had different effect on the cell cycle of the used A2780 cells than **5** and *cisplatin*. Despite different cell cycle perturbation, both complexes **5** and **6** (as well as *cisplatin*) induced apoptosis which predominates over necrosis. Finally, the results showed that p53 is relevant in the mechanism of action of complex **5**, which showed (similarly as *cisplatin*) higher cytotoxicity at the p53-proficient cells (HCT116 $p53^{+/+}$) than at the p53-knockout cells (HCT116 $p53^{-/-}$); HCT116 = human colon carcinoma cells. In contrast, the mechanism of action of complex **6** seems to be independent from the transcription factor p53.

Complexes **5** [32] and **6** [31] were further studied as photoactivatable agents whose cytotoxicity and several intracellular processes can be effectively modified by the UVA irradiation. Cytotoxicity of complexes **5** (IC_{50} > 100 μM in the dark and 9.8 μM after irradiation) and **6** (IC_{50} = 32.3 μM in the dark and 1.4 μM after irradiation) was enhanced by the irradiation of the treated A2780 cells. Complex **5** exhibited the DNA cleavage activity and a potency to unwind DNA double helix when the pSP73 plasmid DNA modified by **5** was irradiated by UVA light [32]. The DNA photocleavage is connected with the singlet oxygen production after the DNA adducts with **5** are irradiated (proved by the electron paramagnetic resonance (EPR) spin-trapping experiments). The UVA irradiation also caused the rearrangement of the DNA adducts with **5**, because *ca.* 2.4-times more interstrand cross-linked DNA was detected after irradiation than in the dark. Finally, the spectroscopic measurements indicated that *1Me*-7aza releases from the structure of complex **5** when irradiated. Concerning the studies performed for complex **6**, the results indicated very similar effects of the UVA light irradiation (increased cytotoxicity, more bifunctional cross-links, *in cellulo* DNA cleavage) [31]. Additionally, binding of **6** to DNA was markedly potentiated when irradiated (quantitative) than in the dark (~2%).

2.2. Diiodido complexes

In the last decade, platinum iodido complexes have been attracting the attention of bioinorganic chemists, because these compounds have shown various advantages (higher activity, different cytotoxic profile, and different mechanism of action) over their chlorido analogues as well as over the clinically used platinum-based drugs [26].

2.2.1. Complexes with 7-azaindole-based ligands

Complex *cis*-[Pt(7aza)$_2$$I_2$] was less toxic ($LD_{50}$ > 400 mg/kg) than its chlorido analogue for the treated rats, however its anticancer effect was similarly low as determined for complex *cis*-[Pt(7aza)$_2$$Cl_2$] [8]. The mentioned iodido complex was later involved in the series of eight *cis*-[Pt(*n*7aza)$_2$$I_2$] complexes, where *n*7aza stands for 7aza, *3Cl*-7aza, *3Br*-7aza, *3I*-7aza, *4Cl*-7aza, *4Br*-7aza (for complex **7**), *5Br*-7aza and 2-methyl-4-chloro-7-azaindole (*2Me4Cl*-7aza; for complex **8**) (Fig. 5, Table 1) [33]. These diiodido complexes were prepared using the stoichiometric reaction of K_2[PtI_4] (prepared *in situ* from K_2[$PtCl_4$] and

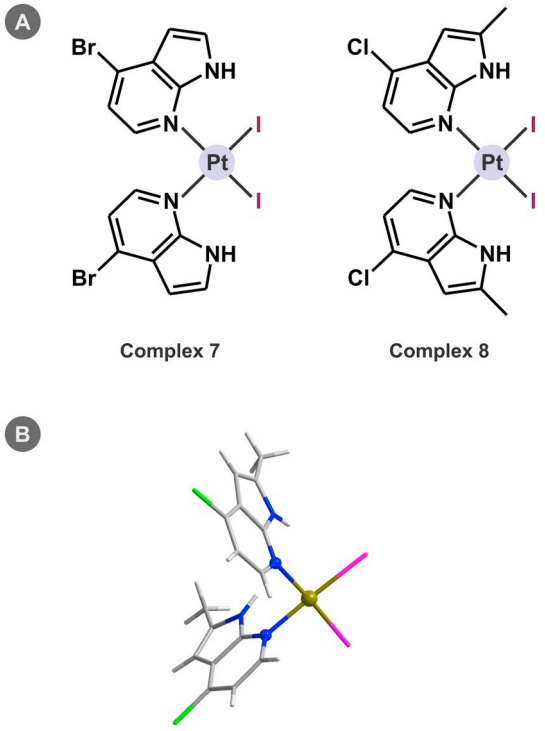

Fig. 5. Structural formulas of *cis*-[Pt(*4Br*-7aza)$_2$I$_2$] (**7**) and *cis*-[PtI$_2$(*2Me4Cl*-7aza)$_2$] (**8**) (**A**; *4Br*-7aza = 4-bromo-7-azaindole, *2Me4Cl*-7aza = 2-methyl-4-chloro-7-azaindole), and the molecular structure of **8**·DMF (DMF molecule of crystallization was omitted for clarity). Structural data were published in [33] (CSD refcode: KEKVOO) (**B**).

an excess of KI) and *n*7aza ligands (24 h, ambient temperature, water/methanol (1:1, *v/v*)). The representative complex **7** was hydrolytically very stable with < 10% hydrolysed after 48 of standing at ambient temperature (20% DMF-d_7/80% D_2O). Additionally to the high hydrolytic stability, complex **7** did not interact with the representative biomolecules GSH and guanosine monophosphate (GMP).

All these complexes exceeded the cytotoxic potency of *cisplatin* at all the used cell lines with the Relative Activity (RA) values equalling to 6.8–47.3 (HOS), 1.6–3.3 (G-361 malignant melanoma), 9.4–17.9 (MCF-7), 4.1–11.6 (A549 lung carcinoma), 4.3–8.0 (22Rv1 prostate carcinoma), 7.6–12.2 (A2780), > 14.3– > 19.2 (A2780R) and > 25.0– > 225.0 (Caco-2 colon carcinoma); RA = IC_{50}(*cisplatin*)/IC_{50}(complex). Complexes *cis*-[Pt(*n*7aza)$_2$I$_2$] were highly effective at various *cisplatin*-sensitive cell lines (*e.g.*, A2780), as well as against the cell lines with either intrinsic (*e.g.*, Caco-2) or acquired (A2780R) resistance towards *cisplatin*. In other words, complexes *cis*-[Pt(*n*7aza)$_2$I$_2$] were able to overcome the resistance of the cancer cells towards the therapeutic action of *cisplatin* (RF = 0.6–1.1 at the A2780/A2780R model). On the other hand, complexes *cis*-[Pt(*n*7aza)$_2$I$_2$] were quite toxic also at the non-cancerous primary culture of human hepatocytes (IC_{50} = 3.8–11.8 μM), thus the selectivity reached the pharmacologically prospective values only in few examples, such as for example SI = 23.8 and 13.6 for **8** at the Caco-2, and HOS cells, respectively.

Flow cytometry studies of the cell cycle modification at the A2780 and MCF-7 cells treated by complexes **7** and **8** proved that effect of these compounds (no cell cycle change induced) differ from *cisplatin* (high S phase populations) [33] as well as from the chlorido analogues (high sub-G_1 phase populations; see above) [30]. In contrast to *cisplatin*, neither complex **7** nor **8** did not change the mobility of pUC19 plasmid DNA, implying that complexes **7** and **8** do not interact covalently with DNA [33], which has to be pointed out as difference not only from *cisplatin* but more importantly also from the chlorido analogues (see above) [30].

Further, the best-performing complexes **7**, **8** and *cis*-[Pt(*4Cl*-7aza)$_2$I$_2$] were also studied for their *in vivo* anticancer activity (L1210 lymphocytic leukaemia model in mice) [33]. Complex **8** improved the mean survival time of the treated mice to the comparable level (T/C = 109%) as *cisplatin* (T/C = 108%); T and C symbolizes the survival times of the treated, and non-treated (control) group, respectively. Again, the T/C of complex **8** was higher than for analogical dichlorido complexes (T/C = 97–100%) studied *in vivo* under the same experimental conditions [30]. The *ex vivo* analysis of the tissues isolated form the treated animals proved complex **8** as the most anticancer effective one in tumour tissues, while its effect at the healthy tissues (spleen and renal) was markedly lower (both comparable with *cisplatin*) [33]. Similarly, to the dichlorido analogues [30], the application of complex **8** decreased the p53 level in the tumour tissues [33]. In connection, complex **8** increased the level of anti-apoptotic protein MCL-1L and active form of Caspase 3. The obtained results pointed out the mechanism of action of the best-performing complex **8** to be different from *cisplatin*, which together with high *in vitro* and *in vivo* anticancer activity favours complex **8** for further pharmacological studies.

2.2.2. Complexes with 4-azaindole-based ligands

With respect to the results obtained for highly cytotoxic dichlorido and especially diiodido complexes with 7aza-based ligands, it was of great interest to investigate similar complexes also with other azaindole isomers (Fig. 1). As the representative one, we chose 4-azaindole (4aza) [18]. Complexes *cis*-[Pt(4aza)$_2$I$_2$] and *cis*-[Pt(*ip*-4aza)$_2$I$_2$] (**9**; Fig. 6) were prepared as described above for the structurally similar complexes **7** and **8** (*i.e.*, reaction of K_2[PtI$_4$] with two molar equivalents of *n*4aza), while the multi-step syntheses of the ammine complexes *cis*-[Pt(4aza)I$_2$(NH$_3$)] and *cis*-[Pt(*ip*-4aza)I$_2$(NH$_3$)] (**10**; Fig. 6) started from K_2[PtCl$_4$], and they were conducted through the intermediates *cis*-[PtI$_2$(NH$_3$)$_2$], *cis*-[PtCl$_2$(NH$_3$)$_2$] (*cisplatin*), NH$_4$[PtCl$_3$(NH$_3$)], K[PtCl$_3$(NH$_3$)] and K[PtI$_3$(NH$_3$)], which finally interacted with 4aza or *ip*-4aza (1-(propan-2-yl)-4-azaindole).

Complexes *cis*-[Pt(*n*4aza)$_2$I$_2$] were hydrolytically stable (20% DMF-d_7/80% D_2O), while complexes *cis*-[Pt(*n*4aza)I$_2$(NH$_3$)] of the second structural type partially hydrolysed in the used medium. Complex **9** also interacted with model proteins cytochrome *c* (1:1 and 1:2 adducts detected) and hen egg-white lysozyme (HEWL; only 1:1 adduct detected). All the complexes exceeded the cytotoxicity of *cisplatin* against the A2780, A2780R and HT-29 (colon carcinoma) (Table 1). The primary culture of human hepatocytes (Hep) was used for the evaluation of toxicity at non-cancerous cells, where the representative complexes *cis*-[Pt(4aza)$_2$I$_2$] (IC_{50} > 100 μM) and **9** (IC_{50} = 38 μM) showed markedly lower activity than at the cancer cells, implying prospective

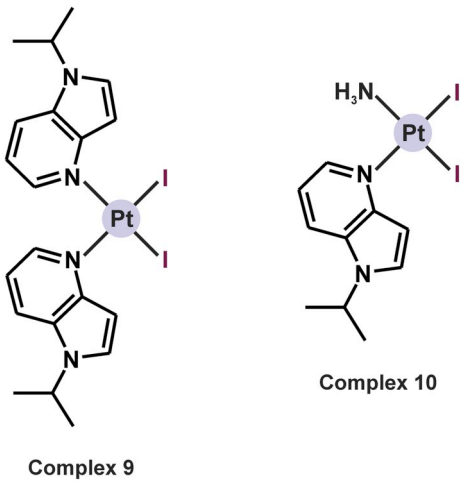

Fig. 6. Structural formulas of *cis*-[Pt(*ip*-4aza)$_2$I$_2$] (**9**) and *cis*-[Pt(*ip*-4aza)I$_2$(NH$_3$)] (**10**); *ip*-4aza = 1-(propan-2-yl)-4-azaindole.

selectivity towards the cancer cells over the normal ones. The resistance factors (RF = 0.8–1.4) revealed the ability of all complexes containing 4aza-based ligands to overcome the acquired resistance against *cisplatin* (A2780/A2780R model). Complexes **9** and **10** induced an increase of G_2/M cell cycle phase populations, as compared with the untreated cells (studied by flow cytometry). Regarding a comparison with 7aza-based complexes (see above), the effect of complex **9** to the A2780 cell cycle is very similar, while it differs markedly from conventional *cisplatin*.

2.3. Carboxylato complexes

2.3.1. Oxalato complexes

Complex [Pt(7aza)$_2$(ox)] was investigated in 1984 for its *in vivo* anticancer activity and despite its toxicity was lower (LD_{50} > 625 mg/kg) as compared with the co-studied dichlorido complex (see above), its therapeutic effect was negligible (T/C = 10.2% at the 625 mg/kg dose; T/C = 11.2% for the control group; T = tumour weight, C = total body weight); ox = oxalato (ethanedioato) [8]. Complex [Pt(7aza)$_2$(ox)] was involved in a series of [Pt(*n*7aza)$_2$(ox)] complexes studied by our group, which was prepared by the reactions of K_2[Pt(ox)$_2$]·2H_2O with *n*7aza ligands, stirred at 50 °C in water/ethanol mixture (1:1, *v/v*) for 48 h; *n*7aza = 7aza, *3Cl*-7aza, *3Br*-7aza (for complex **11**), *3I*-7aza, *4Cl*-7aza, *4Br*-7aza and *5Br*-7aza (Fig. 7) [9,27,34]. However, [Pt(*n*7aza)$_2$(ox)] complexes were inactive up to the highest tested concentration given by their limited solubility, except for [Pt(*3Br*-7aza)$_2$(ox)] (**11**), whose cytotoxicity was even higher as compared with *cisplatin* at some of the used human cancer cell lines (*i.e.*, A2780 ovarian carcinoma or HeLa cervix carcinoma cells; Table 1). Complex **11** was hydrolytically stable and did not interact with the model biomolecules (CySH, GSH, GMP).

2.3.2. Cyclobutane-1,1′-dicarboxylato complexes

Complexes of the general formula [Pt(*n*7aza)$_2$(cbdc)] (*n*7aza = *3Cl*-7aza, *3Br*-7aza, *3I*-7aza, *4Cl*-7aza, *4Br*-7aza (for complex **12**) and *5Br*-7aza (for complex **13**); cbdc = cyclobutane-1,1′-dicarboxylato) represent the derivatives of clinically-used platinum-based drug *carboplatin* (Fig. 7) [35]. These compounds were prepared by the reactions of the above mentioned *cis*-[Pt(*n*7aza)$_2$I$_2$] complexes with silver cyclobutane-1,1′-dicarboxylate in DMF (48 h of stirring in the dark). The cytotoxic activity of [Pt(*n*7aza)$_2$(cbdc)] complexes was higher as compared with *cisplatin* and *carboplatin* at the A2780 cells, and prostate carcinomas LNCaP and PC-3 (Table 1). Interestingly, an improvement of cytotoxic potency can be achieved by the UVA light irradiation (20 min, λ_{max} = 365 nm).

Complexes markedly more platinated double-helical ctDNA (calf thymus DNA) in cell-free experiments when irradiated than in the dark. From the chemical point of view, the UVA irradiation of the representative complex **12** induced a release of the *4Br*-7aza ligand and opening of the Pt-cbdc chelate ring. Complex **12** interacted with GMP but not with GSH after the UVA irradiation. The adducts of **12** with a linear pSP73KB/*Hpa*I DNA fragment inhibited the RNA synthesis (studied *in vitro* using T7 RNA polymerase) more effectively after irradiation than in the dark, although in both cases the DNA adducts were mutually similar and analogical with *cisplatin* (mainly GG and AG sites). Further, complex **12** formed the interstrand DNA cross-links only when irradiated (studied using linear pSP73KB/*Eco*RI DNA). In connection with this observation, results of the fluorescence experiments on the DNA-ethidium bromide (EtBr) adducts indicated the formation of adducts with monofunctional (monodentate-coordinated) complexes in the dark, while the studied complex coordinated DNA bidentately in a *cisplatin*-like manner after irradiation.

2.3.3. Malonato complexes

Complexes [Pt(*3I*-7aza)$_2$(mal)] (**14**) and [Pt(*4Br*-7aza)$_2$(mal)] (**15**), prepared by the reaction of *cis*-[Pt(*n*7aza)$_2$I$_2$] complexes with silver malonate (chloroform, 48 h, in the dark), were moderately effective at the A2780 and A2780R cells (Fig. 7 and Table 1), but they showed different toxicity at the healthy MRC-5 cells (IC_{50} > 50.0 μM, and IC_{50} = 21.9 μM, respectively); mal = malonato (propanedioato), MRC-

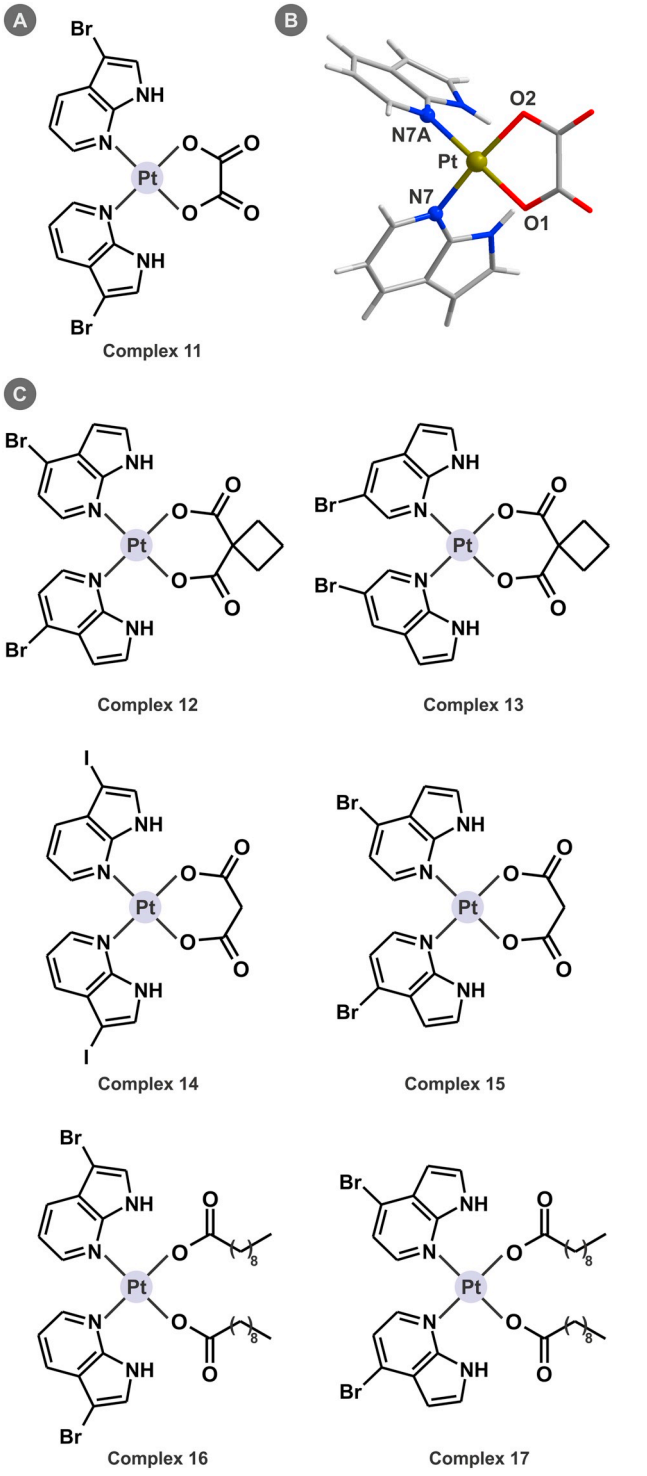

Fig. 7. Structural formula of [Pt(*3Br*-7aza)$_2$(ox)] (**11**; **A**; *3Br*-7aza = 3-bromo-7-azaindole), the molecular structure of [Pt(7aza)$_2$(ox)] (**B**; 7aza = 7-azaindole; structural data were published in [9]; CSD refcode: FAMROC), and structural formulas of [Pt(*4Br*-7aza)$_2$(cbdc)] (**12**), [Pt(*5Br*-7aza)$_2$(cbdc)] (**13**), [Pt(*3I*-7aza)$_2$(mal)] (**14**), [Pt(*4Br*-7aza)$_2$(mal)] (**15**), *cis*-[Pt(*3Br*-7aza)$_2$(dec)$_2$] (**16**) and *cis*-[Pt(*4Br*-7aza)$_2$(dec)$_2$] (**17**) (**C**; *4Br*-7aza = 4-bromo-7-azaindole; *5Br*-7aza = 5-bromo-7-azaindole; *3I*-7aza = 3-iodo-7-azaindole; ox = oxalato (ethanedioato), cbdc = cyclobutane-1,1′-dicarboxylato, mal = malonato (propanedioato) and dec = decanoato.

5 = lung fibroblasts [36]. The resistance factors equal 1.1 (for **14**) and 0.9 (for **15**). The representative complex **15** was hydrolytically stable and did not interact with GMP in the used medium (50% DMF-d_7/50% D_2O). However, the obtained ^{1}H NMR and ESI-MS (electrospray ionisation mass spectrometry) results indicated that **15** induced the oxidation of GSH to glutathione disulfide (GSSG). Complex **15** (log$P$ = −0.71) is slightly more lipophilic than *cisplatin* (log$P$ = −1.52). The application of complex **15** to the A2780 cells led to the enhancement of G_0/G_1 population as compared with non-treated cells, which is different from *cisplatin*.

2.3.4. Decanoato complexes

Complexes *cis*-[Pt(*3Br*-7aza)$_2$(dec)$_2$] (**16**) and *cis*-[Pt(*4Br*-7aza)$_2$(dec)$_2$] (**17**) were studied together with the above-discussed malonato complexes and they were prepared by the similar procedure, specifically by the interaction of the stoichiometric amount of diiodido complexes *cis*-[Pt(*n*7aza)$_2$I$_2$] and silver decanoate ($CHCl_3$, 48 h of stirring in the dark; Fig. 7 and Table 1); dec = decanoato [36]. The ability of decanoato complexes to overcome the acquired resistance towards *cisplatin* was proved by low resistance factors of these agents (RF = 1.0–1.5). Similarly to the malonato complexes **14** and **15**, the decanoato complexes **16** (IC_{50} > 50.0 μM) and **17** (IC_{50} = 26.2 μM) affected differently the viability of non-cancerous MRC-5 cells. Decanoato complex **16** (log$P$ = 0.30) exceeded the lipophilicity of the malonato complex **15**, which correlates with higher cytotoxicity of **16** than observed for **15** (Table 1). The A2780 cells treated by **16** showed high sub-G_1 population that is similar to the dichlorido complexes but differs from the diiodido [33] and malonato [36] complexes containing the 7-aza-based ligands.

2.4. Other types of complexes

Ruiz et al. reported the complexes [Pt(C_6F_5)$_2$(7aza)$_2$], (NBu_4)[Pt(C_6F_5)$_2$(7aza)(7aza$^-$)]·7aza, (NBu_4)$_2$[Pt$_2$(μ-OH)(μ-7aza$^-$)(C_6F_5)$_4$], [Pt(dmba$^-$)(7aza$^-$)(dmso)] (**18**; Fig. 8) and [Pt(dmba$^-$)(7aza$^-$)(PPh_3)]; dmba = *N*,*N*-dimethylbenzylamine, PPh_3 = triphenylphosphane [12].

Among the described complexes, complex (NBu_4)[Pt(C_6F_5)$_2$(7aza)(7aza$^-$)]·7aza has to be highlighted because of the unusual combination of electroneutral N7-coordinated 7aza and deprotonated *N*1-coordinated 7aza$^-$. The best-performing complex **18** was prepared by the reaction of [PtCl(dmba$^-$)(dmso)] and silver perchlorate in acetone (30 min), followed by the treatment with an equimolar amount of 7aza in the presence of excess KOH in methanol for 1 h. Complex **18** revealed submicromolar activity against all the used cell lines (T47D breast carcinoma, A2780, A2780R; Table 1), connected with the ability to overcome the acquired resistance of the A2780 cells against *cisplatin* (RF = 1.3 at the A2780/A2780R model). Additional biological assays indicated that **18** alerted the used DNA models, specifically the calf thymus DNA (circular dichroism spectroscopy studies) and pBR322 plasmid DNA (gel electrophoresis).

This work was followed by two [Pt(7aza^n)Cl(dmba$^-$)] complexes containing *C*,*N*-coordinated dmba$^-$ ligand (analogically with **18**) and N7-coordinated 7aza-based ligand linked through an ethynyl-containing linker with a testosterone or nortestosterone residue (7aza^n) (Fig. 8) [37]. A derivatization of 7aza moiety by a steroidal residue enhanced the accumulation of complex [Pt(7aza^1)Cl(dmba$^-$)] (**19**) bearing the nortestosterone-based ligand 7aza^1 at the T47D, A2780 and A2780R cells as compared with *cisplatin*. Complex **19** was prepared from the starting dinuclear complex [Pt(μ-Cl)(dmba$^-$)]$_2$ using its reaction with two molar equivalents of 7aza^1 at 50 °C for 5 days. The cytotoxic activity of **19** was lower in comparison with the previously reported complex **18** at the T47D, A2780 and A2780R cells (Table 1). However, it showed high ability to overcome the acquired resistance of the used A2780 cells against the biological action of *cisplatin* with RF = 1.1. An explanation of low RF observed for **19** is quite disputable, because although its cellular accumulation was even higher at the A2780R cells than at the A2780 ones, the same was observed also for *cisplatin*, whose activity was significantly lower at the A2780R cells than at the A2780 ones (RF = 8.7). Additionally, the [Pt(7aza^n)Cl(dmba$^-$)] complexes were poorly selective towards the used cancer cells over the normal ones (human LLC-PK1 renal cell line was used).

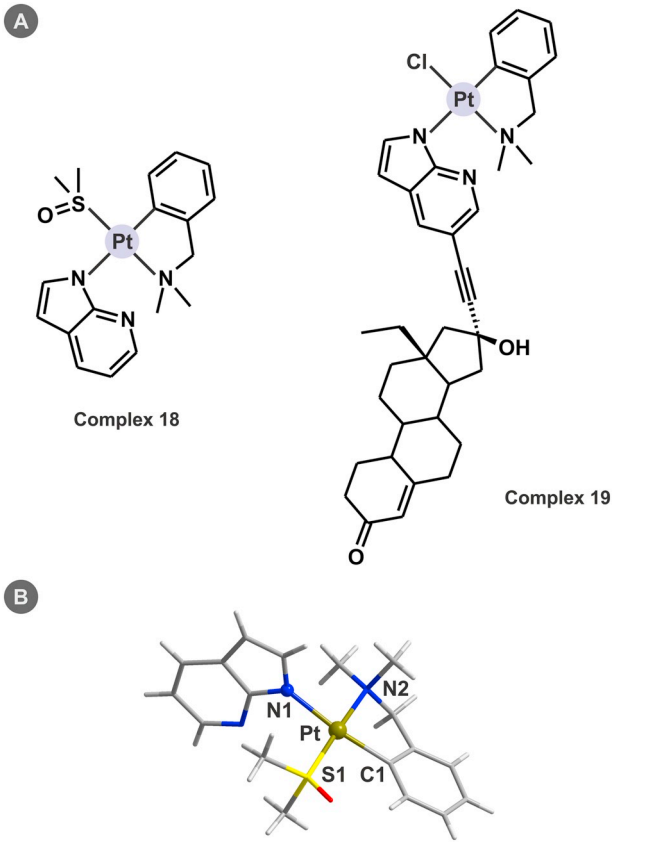

Fig. 8. Structural formulas of [Pt(dmba$^-$)(7aza$^-$)(dmso)] (**18**) and [Pt(7aza^1)Cl(dmba$^-$)] (**19**), where dmba = *N*,*N*-dimethylbenzylamine, aza^1 = 7aza linked with a nortestosterone residue (**A**), and the molecular structure of **18**·1/4tol·1/2H_2O (tol = toluene; tol and H_2O molecules of crystallization were omitted for clarity). Different labels than in deposited CIF files were used, as follows: N1 in the drawing = N2 in the CIF file; N2 = N1). Structural data were published in [12] (CSD refcode HUWJOZ) (**B**).

It has to be noted, that in contrast to complexes **1–17**, whose cytotoxicity was assessed in the presence of DMF [10,11,27,31–35], complexes **18** and **19** were dissolved in DMSO prior the cytotoxicity studies [12,37]. It is known that DMSO affects the cytotoxic activity of various platinum(II) complexes, including *cisplatin*, which showed completely different IC_{50} values when pre-dissolved in DMF (IC_{50} = 5.0 μM) and in DMSO (IC_{50} = 177.6 μM); studied under the same experimental conditions at the DLD1 human colorectal carcinoma cells [38]. Thus, an utilization of DMSO for the biological testing of platinum complexes possibly affects their cytotoxicity (in terms of IC_{50} values summarized in Table 1). However, this is not the case of the discussed complexes **18** and **19** proved to be stable in DMSO (both complexes) or its mixture with 100 mM NaCl in D_2O (studied only for **19**) for at least 24 h at ambient temperature. On the other hand, with respect to the deactivation of *cisplatin* by DMSO (see above), it has to be noted that the RA values given in Table 1 for complexes **18** and **19** can be hardly compared with those obtained for platinum(II) complexes **1–17** studied in DMF, which does not deactivate the used reference drug *cisplatin*.

Complex **19** modified the gel electrophoretic mobility of the pBR322 plasmid DNA, implying their mutual interaction and alternation of the structure of the used DNA model. The results of mass

spectrometry experiment proved the interaction of the [Pt(7aza^{n})Cl(dmba^{-})] complexes with 9-ethylguanine (ESI-MS) and suggested that these complexes interact only with the double stranded (DS) oligonucleotide but not with the single stranded one (electrospray ionisation time-of-flight mass spectrometry (ESI-TOF-MS)). Both complexes acted as effective cathepsin B (catB) inhibitors, following the hypothesis that catB is a possible therapeutic target for various anticancer agents.

Similarly to **19** [37], complex **18** also interacted with DNA models, namely DS oligonucleotides, and either ethidium bromide or Hoechst 33258 displacement experiments from ctDNA [39]. Complex **18** was also proved as a good inhibitor of catB. Furthermore, this work showed that complex **18** interacted with several representative proteins (transferrin, albumin, myoglobin, cytochrome C and mammalian metallothionein (mouse MT1 isoform)), mainly on their surface. The replacement of ligands of **18** was driven by the nature (donor atom) of the interacting amino acid. In particular, complex **18** released either dmso when interacted with cysteine residue, or 7aza in the case of interaction with histidine residue.

3. Ruthenium(II) complexes

Ruthenium complexes are one of the most promising alternatives for the platinum-based drugs [40,41]. They offer various design (*e.g.*, octahedral tetrachlorido complexes, half-sandwich complexes or cyclometalated complexes) and many representatives showed remarkable cytotoxic potency connected with different mechanism of action (*e.g.*, cell redox-status modulation or protein targeting) from the platinum-based chemotherapeutics. The most importantly, Ru(III) complexes NAMI-A (imidazolium *trans*-(dimethyl sulfoxide)(1*H*-imidazole)-tetrachloridoruthenate(III)) and IT-139 (NKP-1339; sodium *trans*-bis(1*H*-indazole)-tetrachloridoruthenate(III)) have entered the clinical trials on human oncological patients [42,43].

Besides Ru(III) complexes, whose biological activation requires intracellular reductive conditions, many types of Ru(II) complexes, which do not face this requirement, were studied for their anticancer activity [40,41]. Regarding the half-sandwich Ru(II) complexes, their design is based on the combination of two labile and one monodentate stable ligands (developed by Dyson and co-workers) [44,45] or the other way around with one bidentate stable ligand and only one labile ligand (developed by Sadler and co-workers) [46].

RAPTA-C, [Ru(η^6-*p*cym)Cl$_2$(pta)] (*p*cym = 1-methyl-4-(propan-2-yl)benzene; pta = 1,3,5-triaza-7-phosphaadamantane), belonging to the first group, was proved as a prospective antimetastatic agent [44,45]. RM175, [Ru(η^6-bph)Cl(en)]PF$_6$ (bph = biphenyl; en = ethane-1,2-diamine) is a typical representative of the second group of half-sandwich complexes containing a bidentate-coordinated ligand [46]. This complex showed promising anticancer activity at the *in vivo* level (well-tolerated, reduced the growth of primary tumours and metastases) [47,48]. The replacement of the chlorido ligand by a bioactive one seems to be reasonable for the development of multi-targeted complexes (*e.g.*, [Ru(η^6-*p*cym)(bphen)(dca)]PF$_6$ dichloroacetato (dca) complex; bphen = 4,7-diphenyl-1,10-phenanthroline (bathophenanthroline)) [49,50]. Furthermore, the requirements of photodynamic therapy were successfully met by cyclometalated complex [Ru(dmbpy)$_2$(iptt)]Cl$_2$ (TLD1433) at the *in vivo* studies as well as in the completed Ib phase of the clinical trials on human oncology patients suffering with non-muscle invasive bladder cancer; dmbpy = 4,4′-dimethyl-2,2′-bipyridine, iptt = 2-(2′,2″:5″,2‴-terthiophene)-imidazo[4,5-*f*][1,10]phenanthroline [51,52].

Among the cytotoxic half-sandwich Ru(II) complexes, a number of dichlorido ones containing one monodentate-coordinated *N*-donor ligand have been reported as highly potent against various human cancer cell lines. In particular, the complexes [Ru(η^6-*p*cym)Cl$_2$(L)], containing mebendazole, clotrimazole, miconazole or ketoconazole as monodentate *N*-donor ligands L, were *in vitro* cytotoxic at the HeLa cells [53]. Similarly designed complexes with pyridine- or triphenylphosphane-based ligands bearing the ethacrynate substituent were moderately potent at the A2780 and A2780R cells [54].

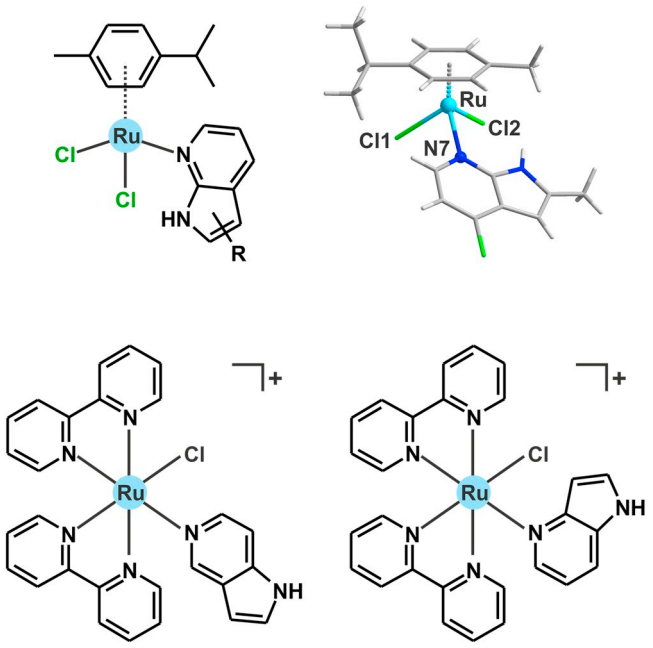

Fig. 9. General structural formula of [Ru(η^6-*p*cym)Cl$_2$(*n*7aza)] complexes, where *n*7aza ligands is represented by 7-azaindole, 3-chloro-7-azaindole, 3-iodo-7-azaindole, 5-fluoro-7-azaindole, 2-methyl-4-chloro-7-azaindole (*2Me4Cl*-7aza), 3-chloro-5-bromo-7-azaindole and 3-iodo-5-bromo-7-azaindole (*top left*), and the molecular structure of [Ru(η^6-*p*cym)Cl$_2$(*2Me4Cl*-7aza)]; *p*cym = 1-methyl-4-(propan-2-yl)benzene. Structural data were published in [55] (CSD refcode: AYEZOV) (*top right*), and the structural formulas of complexes *cis*-[Ru(5aza)(bpy)$_2$Cl]PF$_6$·H$_2$O (*bottom left*) and *cis*-[Ru(4aza)(bpy)$_2$Cl]PF$_6$ (*bottom right*); 4aza = 4-azaindole, 5aza = 5-azaindole, bpy = 2,2′-bipyridine.

We followed this design with a series of [Ru(η^6-*p*cym)Cl$_2$(*n*7aza)] complexes containing 7aza, *3Cl*-7aza, *3I*-7aza, 5-fluoro-7-azaindole (*5F*-7aza), *5Br*-7aza, *2Me4Cl*-7aza, *3Cl5Br*-7aza and *3I5Br*-7aza (Fig. 9) [55]. Complexes [Ru(η^6-*p*cym)Cl$_2$(*n*7aza)] were prepared by a straightforward reaction of [Ru(μ-Cl)(η^6-*p*cym)Cl]$_2$, a typical starting Ru(II) complex for the syntheses of half-sandwich complexes, with two molar equivalents of the appropriate 7aza derivative (methanol, room temperature, 20–180 min). However, these compounds were inactive at the A2780 cells up to the highest tested concentration of 50 μM. The inactivity of complexes is most likely caused by their poor stability in solution, especially in the presence of water, where they decomposed to inactive starting Ru(II) dimer [Ru(μ-Cl)(η^6-*p*cym)Cl]$_2$ and the corresponding *n*7aza ligand.

Complexes *cis*-[Ru(4aza)(bpy)$_2$Cl]PF$_6$ and *cis*-[Ru(5aza)(bpy)$_2$Cl]PF$_6$·H$_2$O (Fig. 9) were prepared by the reaction (2 h under reflux) of *cis*-[RuCl$_2$(bpy)$_2$] and slight excess of 4aza or 5aza in water/ethanol mixture (1:3, *v/v*), followed by an addition of excess NH$_4$PF$_6$ [5]. Both complexes showed lower than 50% inhibition of cell growth at the applied 35 μM concentration (IC$_{50}$ > 35 μM), studied at Ovacar-8 ovarian, SF-295 glioblastoma and HCT-116 cells. Nevertheless, both complexes were designed as prospective metallovasodilators, thus their low cytotoxicity has to be understood as a positive feature in the context of the vasodilatory activity. Among the studied complexes, the highest vasodilatory activity (IC$_{50}$ = 55 nM) was reached by 5aza-containing complex *cis*-[Ru(5aza)(bpy)$_2$Cl]PF$_6$·H$_2$O.

4. Palladium(II) complexes

Palladium(II) complexes are structurally similar with their Pt(II)

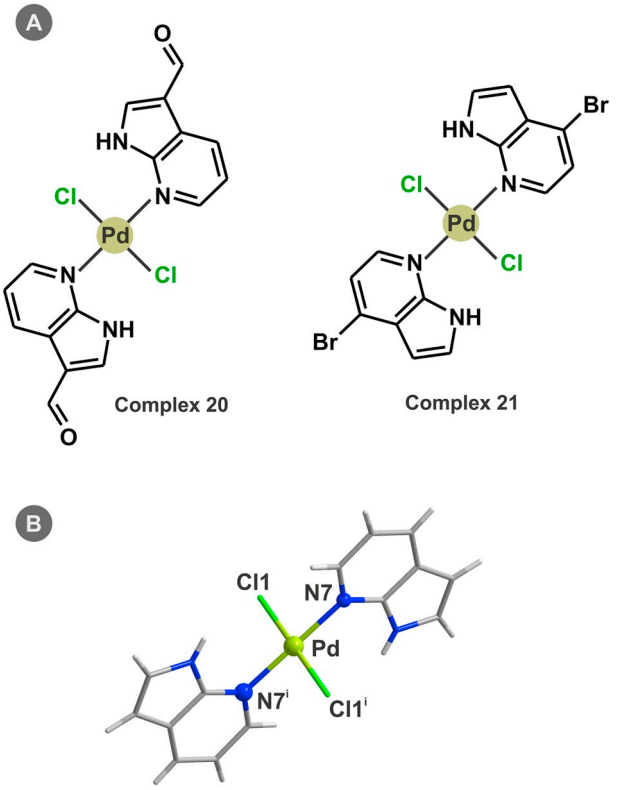

Fig. 10. Structural formulas of *trans*-[Pd(*3Ca*-7aza)$_2$Cl$_2$] (**20**) and *trans*-[Pd(*4Br*-7aza)$_2$Cl$_2$] (**21**) (**A**; *3Ca*-7aza = 7-azaindole-3-carboxaldehyde, *4Br*-7aza = 4-bromo-7-azaindole), and the molecular structure of *trans*-[Pd(7aza)$_2$Cl$_2$]·DMF (7aza = 7-azaindole; DMF molecule of crystallization was omitted for clarity). Symmetry code: (i) 1-x, 1-y, 1-z. Structural data were published in [13] (CSD refcode: LUXFER) (**B**).

analogues, however their lower stability (*e.g.*, rapid isomerization) and higher kinetic lability (*e.g.*, inactivation by various biomolecules) prevent their pharmacological utilization [56]. Nevertheless, a number of Pd(II) complexes have been reported to date as being highly *in vitro* cytotoxic at various human cancer cell lines, including those known to be resistant to platinum-based drugs [57].

Concerning Pd(II) complexes containing 7aza-based ligands, complexes *trans*-[Pd(*3Ca*-7aza)$_2$Cl$_2$] (**20**; Fig. 10), *trans*-[Pd(*4Cl*-7aza)$_2$Cl$_2$], *trans*-[Pd(*4Br*-7aza)$_2$Cl$_2$] (**21**; Fig. 10) and *trans*-[Pd(*3Br4Cl*-7aza)$_2$Cl$_2$] were studied for their cytotoxicity at the T47D, MCF-7, A549 and A2780 cells, where these complexes were markedly less potent than *cisplatin*, except for **20** whose activity was higher than for *cisplatin* at the T47D cell line (Table 1); *3Ca*-7aza = 7-azaindole-3-carboxaldehyde, *3Br4Cl*-7aza = 3-bromo-4-chloro-7-azaindole [58,59]. However, the toxicity of these complexes, including **20**, at the BALB/3 T3 normal mouse fibroblast was comparable with the efficacy at the used cancer cells, implying their low selectivity towards the cancer cells over the healthy ones. Regarding synthesis of *trans*-[Pd(*n*7aza)$_2$Cl$_2$] complexes, it was analogical with the synthesis of the above-mentioned platinum (II) dichlorido complexes. In particular, $K_2[PdCl_4]$ were stirred with two molar equivalents of *n*7aza ligand in water/ethanol mixture at 50 °C for 48 h. It has to be noted that complexes **20** and **21** were studied in the presence of DMSO, possibly affecting their biological activity [38]. However, the stability studies in DMSO-containing media were not performed for these complexes, leaving the question of the DMSO effect on the potency of **20** and **21** unanswered.

5. Iridium(III) complexes

In the field of iridium bioinorganic chemistry, half-sandwich [60] and cyclometalated [61] complexes are widely studied as pharmacologically prospective, since many representatives have been reported as highly anticancer active at both the *in vitro* and *in vivo* level. Half-sandwich Ir(III) complexes act through the redox mechanisms of action, that is different from platinum-based drugs, which favour Ir(III) complexes of this type for further studies and underline their therapeutic potential [62].

With respect to the successful utilization of 7aza-based ligands for the studies of Pt(II) complexes (see above) [27–33], we have tended to study non-platinum half-sandwich complexes containing 7-aza-based ligands. However, the results obtained for [Ru(η^6-*p*cym)Cl$_2$(*n*7aza)] complexes (inactivity, poor stability in solution) [55] and their [Ir(η^5-Cp*)Cl$_2$(*n*7aza)] analogues (P. Štarha and Z. Trávníček, manuscript in preparation; Cp* = pentamethylcyclopentadienyl), led us to the preparation of 7aza derivatives suitable to act as bidentate ligands chelating the used metal of the [M(η-ar)(*n*7aza)Cl]$^{0/+}$ type of complexes.

A series of six complexes of the general formula [Ir(η^5-Cp^x)(*n*7aza$^{-/0}$)Cl]$^{0/+}$ was obtained by the reactions of either [Ir(μ-Cl)(η^5-Cp*)Cl]$_2$ or [Ir(μ-Cl)(η^5-Cp^{ph})Cl]$_2$ with *py*-7aza, 1-phenyl-7-azaindole or 1-(thiophen-2-yl)-7-azaindole (*th*-7aza) in methanol; Cp^x = Cp* or 1,2,3,4-tetramethyl-5-phenylcyclopentadienyl (Cp^{ph}) [63]. The best-performing complex [Ir(η^5-Cp^{ph})(*py*-7aza)Cl]PF$_6$ (**22**; Fig. 11) exceeded the *in vitro* cytotoxicity of *cisplatin* at several of the used cancer cell lines (Table 1), while its activity was markedly lower at the non-cancerous MRC-5 cells (IC$_{50}$ > 50 μM), indicating high selectivity of **22** towards cancer cells over the normal ones. For the first time in the field of half-sandwich Ir(III) complexes, the cytotoxicity was studied at the advanced model based on the spheroid cancer cell culture (MCF-7 cells were used). High cytotoxic potency of **22** even at the used 3D culture (IC$_{50}$ = 22.9 μM for **22** and 35.4 μM for *cisplatin*) highlighted its high potential towards the further studies including *in vivo* anticancer activity. Regarding the mechanism of action, lipophilic complex **22** was *ca.* 250-times more accumulated at the A2780 cells than *cisplatin* and

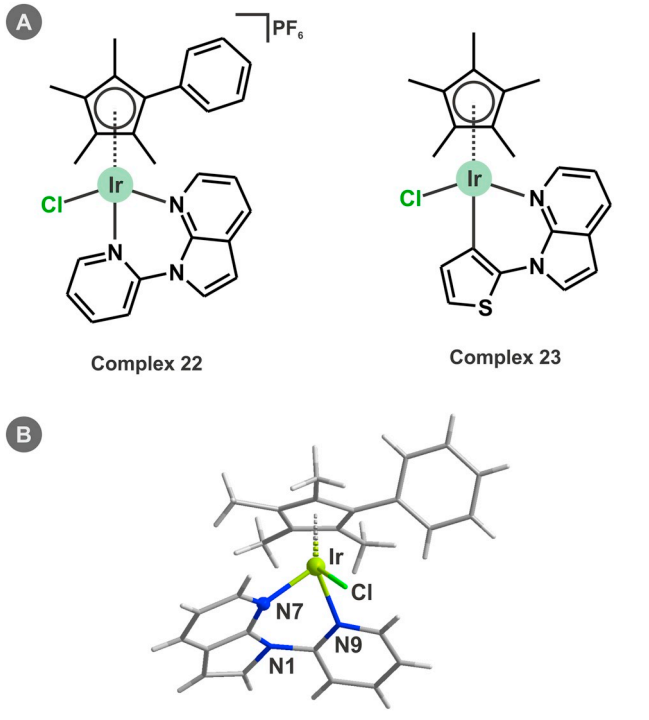

Fig. 11. Structural formulas of [Ir(η^5-Cp^{ph})(*py*-7aza)Cl]PF$_6$ (**22**) and [Ir(η^5-Cp*)(*th*-7aza$^-$)Cl] (**23**) (**A**; *py*-7aza = 1-(pyridin-2-yl)-7-azaindole, *th*-7aza = 1-(thiophen-2-yl)-7-azaindole, Cp^{ph} = 1,2,3,4-tetramethyl-5-phenylcyclopentadienyl, Cp* = pentamethylcyclopentadienyl), and the molecular structure of **22** (PF$_6$ anion was omitted for clarity). Structural data were published in [63] (CSD refcode SIKXOC) (**B**).

affected the A2780 cell cycle (G_0/G_1 arrest) differently than *cisplatin* (increase of G_2/M cell cycle phase population). Other studied complexes, such as the electroneutral complex [Ir(η^5-Cp*)(*th*-7aza$^-$)Cl] (**23**; Fig. 11 and Table 1), were markedly less effective than **22**.

6. Gold(I) complexes

Several gold(I) compounds, such as the best-known *Auranofin* (triethylphosphane-(2,3,4,6-tetra-*O*-acetyl-β-*D*-thiopyranosato)gold(I) complex) are being used as a special type of anti-inflammatory drugs (in so called chrysotherapy) [64]. However, *Auranofin* and many others gold(I) complexes have been reported as having high and pharmacologically prospective anticancer activity [65,66]. Currently, *Auranofin* is under the clinical investigation as prospective anticancer drug for human oncology.

Triphenylphosphane complexes of the general formula [Au(*n*7aza$^-$)(PPh_3)] were prepared by a one-step synthesis of [AuCl(PPh_3)] with a slight excess of *n*7aza in the presence of NaOH (in acetone, 48 h, 50 °C), and they were studied for their *in vitro* cytotoxicity at the A2780 cells and their variant with the acquired resistance against *cisplatin* (A2780R); *n*7aza = 7aza, *3Cl*-7aza, *3Br*-7aza, *3I*-7aza, *5Br*-7aza (for complex **24**), *3Cl5Br*-7aza, *3I5Br*-7aza and *2Me4Cl*-7aza (for complex **25**) (Fig. 12, Table 1) [67]. Besides the considerably higher *in vitro* cytotoxicity in comparison with *cisplatin*, the studied Au(I) complexes **24** and **25** showed the promising selectivity because their activity was several times lower at the normal MRC-5 cells (IC_{50} = 26.0 μM and 26.9 μM for **24**, and **25**, respectively) than at the used cancer cells. The ^{1}H and ^{31}P NMR, and ESI-MS solution behaviour studies indicated high hydrolytic stability of the representative complex **25**, but the release of *2Me4Cl*-7aza ligand from the structure of complex **25** was observed in the presence of the representative biomolecules GSH, CySH and bovine serum albumin.

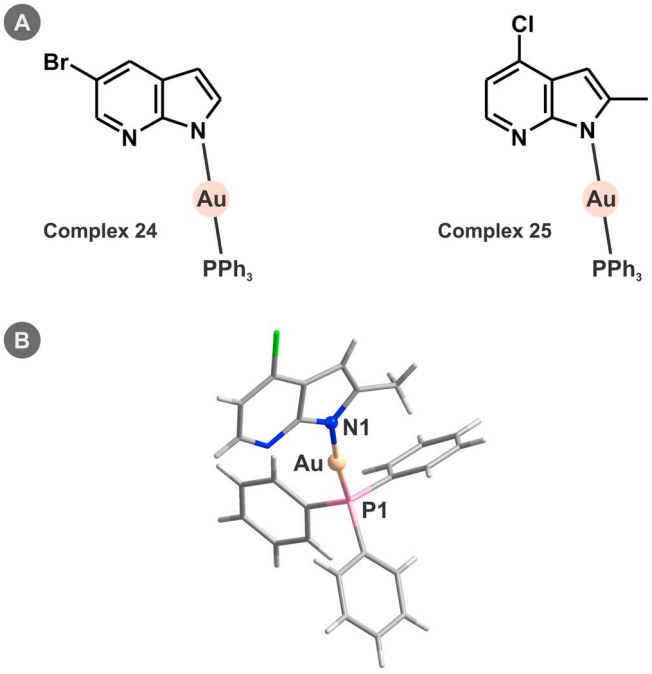

Fig. 12. Structural formulas of [Au(*5Br*-7aza$^-$)(PPh_3)] (**24**) and [Au(*2Me4Cl*-7aza$^-$)(PPh_3)] (**25**) (**A**; *5Br*-7aza = 5-bromo-7-azaindole, *2Me4Cl*-7aza = 2-methyl-4-chloro-7-azaindole, PPh_3 = triphenylphosphane), and the molecular structure of **25**·1/2H_2O (H_2O molecule of crystallization was omitted for clarity). Structural data were published in [67] (CSD refcode KEKWOP) (**B**).

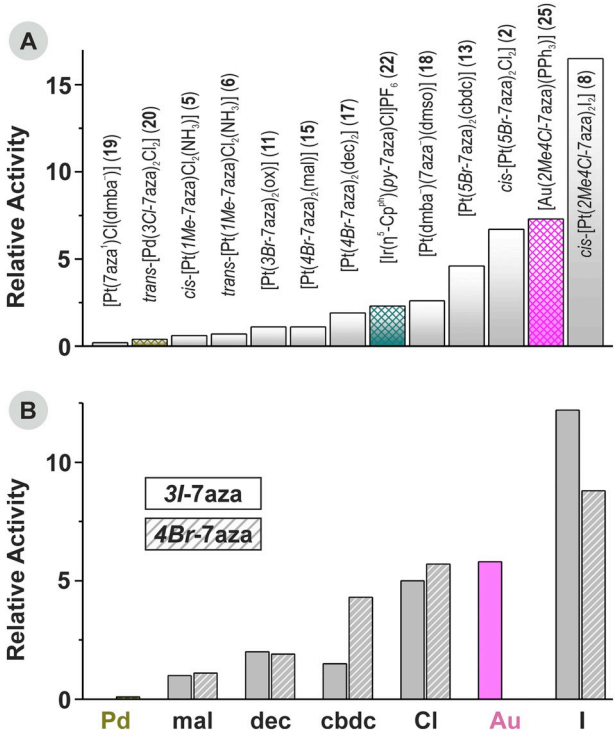

Fig. 13. A comparison of the Relative Activity values calculated form the IC_{50} values (**A**) of the representative complexes showing the highest activity at the A2780 human ovarian carcinoma cells within the specified structural types, and (**B**) for the specified structural types containing either 3-iodo-7-azaindole (*3I*-7aza) or 4-bromo-7-azaindole (*4Br*-7aza) (studied also at the A2780 cells). Relative Activity = IC_{50}(*cisplatin*)/IC_{50}(complex).

7. Structure-activity relationship

7.1. Types of complexes

Obviously, the type of complex, in which the azaindole-based ligand is coordinated, is a crucial factor driving the resulting biological activity. A detail analysis of the published results (IC_{50} values were recalculated to Relative Activity = IC_{50}(*cisplatin*)/IC_{50}(complex)) showed relevant differences between the studied types of complexes (Fig. 13). Within Fig. 13A, the best-performing *n*7aza-containing complexes are given for each structural type overviewed in this work, as resulted from the *in vitro* cytotoxicity testing at the A2780 human cancer cell line, showing the Pt(II) diiodido complexes [33] as the highest active type of complexes containing the 7aza-based ligands, followed by Au(I) triphenylphosphane [67] and Pt(II) dichlorido [28,29] complexes. Further, the dependence of *in vitro* cytotoxicity on the structural type of 7aza-based complex is more or less identical for the best-performing complexes within the studied structural types (Fig. 13A) as well as for representatives containing the same 7aza derivatives, namely *3I*-7aza and *4Br*-7aza (Fig. 13B).

Because Pt(II) dichlorido [28,29] and diiodido [33] complexes were studied with similar library of 7aza derivatives and at similar human cancer cell lines, a deeper comparison of the results obtained for these two structural types can be made (Fig. 14). Indeed, most of diiodido complexes showed higher activity at most of the used cell lines, as compared with the dichlorido analogues. Among them, complexes *cis*-[Pt(*3Cl*-7aza)$_2$$I_2$] and *cis*-[Pt(*4Br*-7aza)$_2$$I_2$] can be highlighted as exceeding their dichlorido counterparts at all of the used human cancer cell lines. On the other hand, all the diiodido complexes exceeded the dichlorido ones at the ovarian, lung, cervical and prostate carcinomas. In the case of osteosarcoma, malignant melanoma and breast carcinoma, some of the studied dichlorido complexes were more cytotoxic

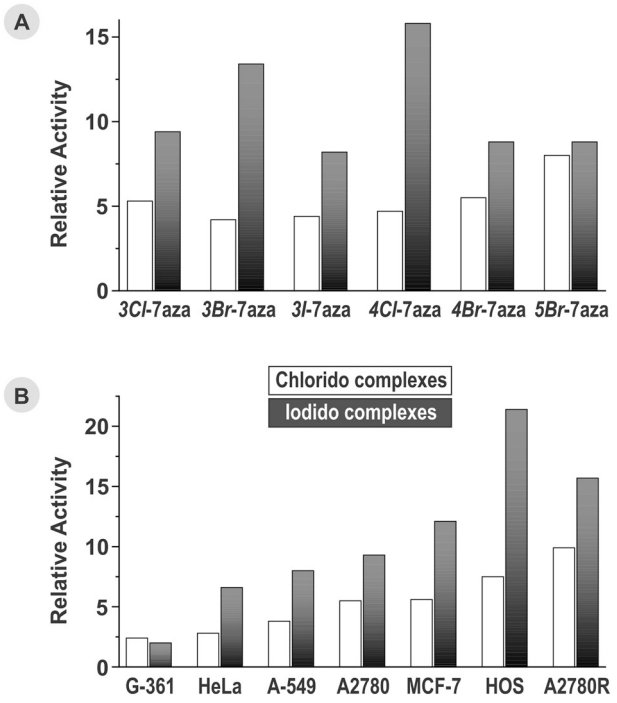

Fig. 14. A comparison of the average Relative Activity values calculated form the IC_{50} values for (**A**) *cis*-[Pt(*n*7aza)$_2$Cl$_2$] and *cis*-[Pt(*n*7aza)$_2$I$_2$] complexes containing the specified *n*7aza ligands studied at the A2780, A2780R, HOS, G-361, MCF-7, A549 and HeLa cells, and (**B**) for *cis*-[Pt(*n*7aza)$_2$Cl$_2$] and *cis*-[Pt(*n*7aza)$_2$I$_2$] complexes at the specified human cancer cell lines. Relative Activity = IC_{50}(*cisplatin*)/IC_{50}(complex), *3Cl*-7aza = 3-chloro-7-azaindole, *3Br*-7aza = 3-bromo-7-azaindole, *3I*-7aza = 3-iodo-7-azaindole, *4Cl*-7aza = 4-chloro-7-azaindole, *4Br*-7aza = 4-bromo-7-azaindole, *5Br*-7aza = 5-bromo-7-azaindole, A2780 = human ovarian carcinoma, A2780R = *cisplatin*-resistant ovarian carcinoma, HOS = osteosarcoma, G-361 = malignant melanoma, MCF-7 = breast adenocarcinoma, A549 = lung carcinoma, HeLa = cervix carcinoma.

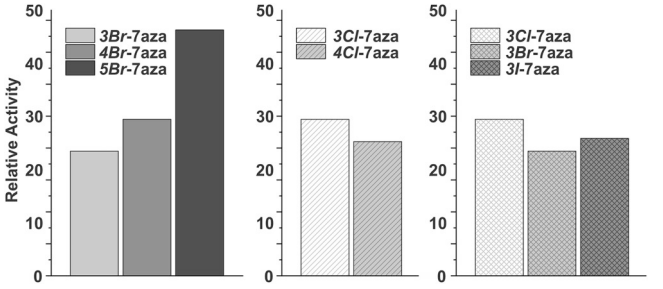

Fig. 15. A comparison of the Relative Activity values calculated form the IC_{50} values of *cis*-[Pt(*n*7aza)$_2$Cl$_2$] complexes containing bromo derivatives (*left*), chloro derivatives (*middle*) or C3-derivatives (*right*) of 7-azaindole. 3-chloro-7-azaindole (*3Cl*-7aza), 3-bromo-7-azaindole (*3Br*-7aza), 3-iodo-7-azaindole (*3I*-7aza), 4-chloro-7-azaindole (*4Cl*-7aza), 4-bromo-7-azaindole (*4Br*-7aza; for complex **2**) or 5-bromo-7-azaindole (*5Br*-7aza; for complex **3**). Relative Activity = IC_{50}(*cisplatin*)/IC_{50}(complex).

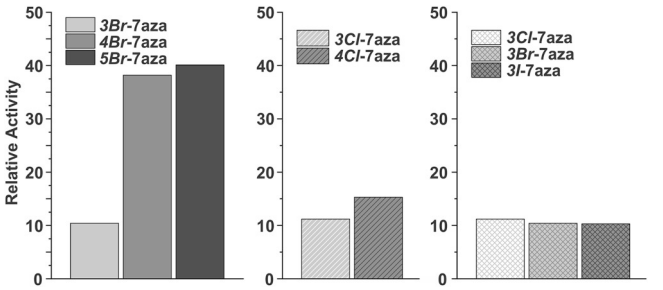

Fig. 16. A comparison of the Relative Activity values calculated form the IC_{50} values of *cis*-[Pt(*n*7aza)$_2$I$_2$] complexes containing bromo derivatives (*left*), chloro derivatives (*middle*) or C3-derivatives (*right*) of 7-azaindole. 3-chloro-7-azaindole (*3Cl*-7aza), 3-bromo-7-azaindole (*3Br*-7aza), 3-iodo-7-azaindole (*3I*-7aza), 4-chloro-7-azaindole (*4Cl*-7aza), 4-bromo-7-azaindole (*4Br*-7aza; for complex **2**) or 5-bromo-7-azaindole (*5Br*-7aza; for complex **3**). Relative Activity = IC_{50}(*cisplatin*)/IC_{50}(complex).

than their diiodido analogues.

Further, a different sensitivity of various cancer cell lines towards the used *cis*-[Pt(*n*7aza)$_2$Cl$_2$] and *cis*-[Pt(*n*7aza)$_2$I$_2$] complexes should be noted, because it highlights a mechanistic difference of these agent and conventional *cisplatin*. Both types of *n*7aza-containing complexes, and especially diiodido ones with RA > 5 at almost all the used cell lines, showed considerable potency at the human cancer cells known to be either sensitive (*e.g.*, HeLa cells) or resistant (*e.g.*, HOS cells) towards the biological effect of *cisplatin* (Fig. 14B).

7.2. Azaindole ring substitution: C-derivatives

Because several 7aza derivatives with the same substituent at different positions (*3Br*-7aza, *4Br*-7aza and *5Br*-7aza), and with different substituents at the same position (*3Cl*-7aza, *3Br*-7aza and *3I*-7aza) were used for the preparation of *cis*-[Pt(*n*7aza)$_2$Cl$_2$] complexes (Section 2.1.1), it was of interest to analyse whether there is a rational relationship between the cytotoxicity and mentioned chemical modifications. In the case of complexes containing bromo derivatives, the *in vitro* cytotoxicity (at most of the studied cell lines) followed the following order: *3Br*-7aza (mean IC_{50} = 7.8 μM; mean RA = 3.9) < *4Br*-7aza (mean IC_{50} = 5.2 μM; mean RA = 4.9) < *5Br*-7aza (mean IC_{50} = 2.5 μM; mean RA = 7.7) (Fig. 15). However this trend was not observed for the complexes with chloro-derived 7aza ligands *3Cl*-7aza (mean IC_{50} = 3.7 μM; mean RA = 4.9) and *4Cl*-7aza (mean IC_{50} = 6.1 μM; mean RA = 4.2) (Fig. 15). Regarding the complexes containing the 7aza-based ligands with differently (Cl, Br and I) substituted C3 position, the mean RA values are more or less comparable (see above and mean RA = 4.3 for *3I*-7aza) with no clear relationship between cytotoxicity and type of C3-substituent (Fig. 15).

The same analysis can be performed also for diiodido complexes of the *cis*-[Pt(*n*7aza)$_2$I$_2$] type (Figs. 5 and 16, Table 1) [33]. Again, complexes containing *4Br*-7aza and *5Br*-7aza were more effective than their analogue with *3Br*-7aza. On the other hand, complexes containing differently substituted *C*3 position of the 7aza ring (*i.e.*, *3Cl*-7aza, *3Br*-7aza and *3I*-7aza) showed more or less similar cytotoxicity with almost identical average RA values obtained on the used panel of human cancer cell lines (Fig. 16).

Concerning the Pd(II) complexes of the *trans*-[Pd(*n*7aza)$_2$Cl$_2$] type, various 7aza derivatives were used [58,59]. The most active complex **20**, containing *3Ca*-7aza, exceeded markedly the cytotoxicity of other complexes containing different halogeno derivatives (namely *4Cl*-7aza, *4Br*-7aza and *3Br4Cl*-7aza) at the used human cancer cell lines, as exemplified in Table 1 for complex **21**. In particular, the IC_{50} values equalled 3.7 μM (for **20**) and 30.3 μM (for **21**) at the A2780 cells. Similar differences were observed at other used cell lines (T47D, MCF-7, A-549), including the non-cancerous BALB/3T3, indicating that the variation of 7aza derivatives in this type of Pd(II) complexes affects not only cytotoxicity but also toxicity at normal cells.

7.3. Azaindole ring substitution: N1-derivatives

Another approach aiming to the improvement of activity of Pt(II) complexes is based on the substitution of the *N*1 position. Interestingly, it has been observed for all the studied types of complexes applying this approach that the replacement of the acidic *N*1−H hydrogen by either methyl or propan-2-yl (isopropyl) led to enhanced cytotoxic activity at

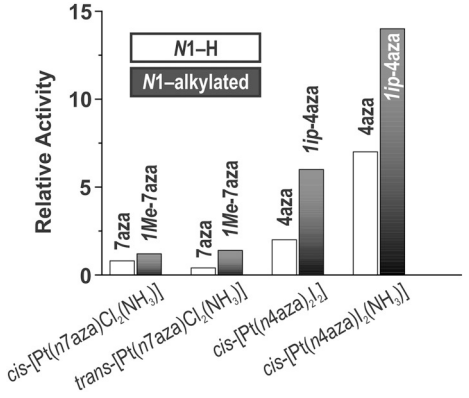

Fig. 17. A comparison of the Relative Activity values calculated form the IC_{50} values of *cis*-[Pt(7aza)Cl_2(NH_3)] (**3**), *trans*-[Pt(7aza)Cl_2(NH_3)] (**4**), *cis*-[Pt(*1Me*-7aza)Cl_2(NH_3)] (**5**), *trans*-[Pt(*1Me*-7aza)Cl_2(NH_3)] (**6**), *cis*-[Pt(4aza)I_2(NH_3)], *cis*-[Pt(*ip*-4aza)I_2(NH_3)] (**10**), *cis*-[Pt(4aza)$_2I_2$] and *cis*-[Pt(*ip*-4aza)$_2I_2$] (**9**); 7aza = 7-azaindole, *1Me*-7aza = 1-methyl-7-azaindole, 4aza = 4-azaindole and *ip*-4aza = 1-(propan-2-yl)-4-azaindole. Relative Activity = IC_{50}(*cisplatin*)/IC_{50}(complex).

the A2780 cells (Fig. 17). The IC_{50} values are given in Table 1 for the pairs of *cis*-[Pt(*n*7aza)Cl_2(NH_3)] (**3** and **5**) and *trans*-[Pt(*n*7aza)Cl_2(NH_3)] (**4** and **6**) complexes [10,11]. In the case of complexes containing 4aza and its *N*1-derivative *ip*-4aza, 4aza-based complexes *cis*-[Pt(4aza)$_2I_2$] and *cis*-[Pt(4aza)I_2(NH_3)] were less effective at the A2780 (IC_{50} = 7.7 and 26.1 μM, respectively) and A2780R (IC_{50} = 8.9 and 32.4 μM, respectively) cells, than their *ip*-4aza analogues having IC_{50} = 3.8 and 2.9 μM, respectively (for **9**) and IC_{50} = 8.9 and 12.1 μM, respectively (for **10**) (Fig. 17) [18]. Also of interest, the results indicated a positive effect of 4aza ring *N*1-alkylation on the cellular accumulation of the complexes under investigation. On the other hand, a comparison of toxicity of complexes *cis*-[Pt(4aza)$_2I_2$] (IC_{50} > 100 μM) and *cis*-[Pt(*ip*-4aza)$_2I_2$] (IC_{50} = 38 μM) suggested that the sensitivity of healthy cells increased along with that of the used cancer cells.

7.4. Geometry of Pt(II) complexes (cis- vs. trans-isomers)

Only two pairs of *cis*- and *trans*-isomers of cytotoxic complexes containing azaindole-based ligands have been reported to date, specifically complexes *cis*-[Pt(7aza)Cl_2(NH_3)] (**3**) and *trans*-[Pt(7aza)Cl_2(NH_3)] (**4**), and their analogues **5** and **6** containing 1-methyl-7-azaindole instead of unsubstituted 7aza (Fig. 17, Table 1) [10,11]. However, the results reported for these structurally similar complexes are in contradiction, because **3** is more cytotoxic than its *trans*-isomer **4** at the used A2780 cells (see Table 1), but *cis*-complex **5** exhibited lower potency than its *trans*-isomer **6** at a panel of human cancer cells (A2780, A2780R, MCF-7, HCT-116 (both $p53^{+/+}$ and $p53^{-/-}$ variants)). However, the cytotoxicity of **5** (IC_{50} = 17 μM) was higher than observed for **6** (IC_{50} = 51 μM) also at the normal primary skin fibroblasts. Other biological differences between the deeply studied complexes **5** and **6** are discussed above (Section 2.1.2).

7.5. Different azaindoles

To answer the question, whether the utilization of some azaindole isomer is more beneficial for the preparation of cytotoxic transition metal complexes, insufficient amount of biological data has been reported in the literature to date. In particular, only a pair of *cis*-[Pt(4aza)$_2I_2$] and *cis*-[Pt(7aza)$_2I_2$] complexes represents two cytotoxic isomers differing in a type of azaindole isomer, which can be compared from the biological point of view. It can be stated that 4aza-based complex *cis*-[Pt(4aza)$_2I_2$] (RA ~3.5 and > 5.6) is less effective than its 7aza-based analogue, *cis*-[Pt(7aza)$_2I_2$] with the RA values of 8.0 and > 15.2 (both complexes studied at the A2780, and A2780R cells, respectively). Importantly, a comparison of toxicity of complexes *cis*-[Pt(7aza)$_2I_2$] (IC_{50} = 3.9 μM) and *cis*-[Pt(4aza)$_2I_2$] (IC_{50} > 100 μM) at the Hep cells suggests a positive effect of the replacement of 7aza with 4aza on the toxicity of the studied diiodido complexes at non-cancerous cells.

8. Conclusions

This work reviews a group of transition metal complexes containing 7-azaindole (7aza), 4-azaindole (4aza), 5-azaindole (5aza) or their derivatives, whose cytotoxicity was studied either *in vitro* or *in vivo*. The published findings revealed that some of these complexes show significant *in vitro* cytotoxicity against a panel of human cancer cell lines and moderate or insignificant toxicity on healthy cells. Moreover, the positive findings following from *in vitro* experiments were also supported by the results on *in vivo* models. It may be concluded that *cis*-diiodidoplatinum(II) complexes containing various 7aza- or 4aza-based ligands represent the most promising ones within the reviewed compounds, revealing in some cases, such as complex *cis*-[PtI_2(*2Me4Cl*-7aza)$_2$] (*2Me4Cl*-7aza = 2-methyl-4-chloro-7-azaindole), extraordinarily higher *in vitro* cytotoxicity at a panel of human cancer cell lines and slightly better *in vivo* anticancer activity as compared with *cisplatin*. In addition, the results of the studies of various processes connected with a mechanism of action indicated a mechanistic difference of these platinum(II)-diiodido complexes, as compared with their dichlorido analogues as well as with *cisplatin*.

Table of abbreviations

1Me-7aza	1-methyl-7-azaindole
2Me4Cl-7aza	2-methyl-4-chloro-7-azaindole
3Br-7aza	3-bromo-7-azaindole
3Br4Cl-7aza	3-bromo-4-chloro-7-azaindole
3Ca-7aza	7-azaindole-3-carboxaldehyde
3Cl-7aza	3-chloro-7-azaindole
3Cl5Br-7aza	3-chloro-5-bromo-7-azaindole
3I-7aza	3-iodo-7-azaindole
3I5Br-7aza	3-iodo-5-bromo-7-azaindole
4aza	4-azaindole (1*H*-pyrrolo[3,2-*b*]pyridine)
4Br-7aza	4-bromo-7-azaindole
4Cl-7aza	4-chloro-7-azaindole
5aza	5-azaindole (1*H*-pyrrolo[3,2-*c*]pyridine)
5Br-7aza	5-bromo-7-azaindole
6aza	6-azaindole (1*H*-pyrrolo[2,3-*c*]pyridine)
7aza	7-azaindole (1*H*-pyrrolo[2,3-*b*]pyridine)
A549	human lung carcinoma cell line
A2780	human ovarian carcinoma cell line
A2780R	*cisplatin*-resistant human ovarian carcinoma cell line
BALB/3T3	normal mouse fibroblasts
bpy	2,2′-bipyridine
Caco-2	human colon carcinoma cell line
cbdc	cyclobutane-1,1′-dicarboxylato
Cp*	pentamethylcyclopentadienyl
Cp^{ph}	1,2,3,4-tetramethyl-5-phenylcyclopentadienyl
dec	decanoato
dmba	*N*,*N*-dimethylbenzylamine
ESI-MS	electrospray ionisation mass spectrometry
G-361	human malignant melanoma cell line
HCT116	human colon carcinoma cell line
HeLa	human cervix carcinoma cell line
HOS	human osteosarcoma cell line
HT-29	human colon carcinoma cell line
IC_{50}	half maximal inhibitory concentration
ip-4aza	1-(propan-2-yl)-4-azaindole
LD_{50}	amount of a substance required to kill half of tested animals

LNCaP	human prostate carcinoma cell line
mal	malonato (propanedioato)
MCF-7	human breast adenocarcinoma cell line
MRC-5	human lung fibroblasts
ox	oxalato (ethanedioato)
PC-3	human prostate carcinoma cell line
PPh_3	triphenylphosphane
py-7aza	1-(pyridin-2-yl)-7-azaindole
RA	Relative Activity (defined as IC_{50}(*cisplatin*)/IC_{50}(complex))
RF	Resistance Factor (defined as IC_{50}(resistant cells)/ IC_{50}(sensitive cells))
SI	Selectivity Index (defined as the ratio of IC_{50}(healthy cells)/ IC_{50}(cancer cells))
T47D	human breast carcinoma cell line

Acknowledgement

The authors gratefully thank the Ministry of Education, Youth and Sports of the Czech Republic (project LO1305) for the financial support.

Notes

Conflicts of interest: none.

References

[1] T. Irie, M. Sawa, Chem. Pharm. Bull. 66 (2018) 29–36.
[2] W. Lee, J.J. Crawford, I. Aliagas, L.J. Murray, S. Tay, W.R. Wang, C.E. Heise, K.P. Hoeflich, H. La, S. Mathieu, R. Mintzer, S. Ramaswamy, L. Rouge, J. Rudolph, Bioorg. Med. Chem. Lett. 26 (2016) 3518–3524.
[3] M.C. Bryan, J.R. Falsey, M. Frohn, A. Reichelt, G. Yao, M.D. Bartberger, J.M. Bailis, L. Zalameda, T. San Miguel, E.M. Doherty, J.G. Allen, Bioorg. Med. Chem. Lett. 23 (2013) 2056–2060.
[4] H.Y. Lee, S.L. Pan, M.C. Su, Y.M. Liu, C.C. Kuo, Y.T. Chang, J.S. Wu, C.Y. Nien, S. Mehndiratta, C.Y. Chang, S.Y. Wu, M.J. Lai, J.Y. Chang, J.P. Liou, J. Med. Chem. 56 (2013) 8008–8018.
[5] D.S. Sá, A.F. Fernandes, C.D.S. Silva, P.P.C. Costa, M.C. Fonteles, N.R.F. Nascimento, L.G.F. Lopes, E.H.S. Sousa, Dalton Trans. 44 (2015) 13633–13640.
[6] I. Holmes, A. Naylor, D. Alber, J.R. Powell, M.R. Major, G. Negoita-Giras, D.R. Allen, L.J. Guetzoyan, N.P. King, N.A. Chapman, Patent Application WO 2017/093545 A1 (2017).
[7] S.B. Zhao, S. Wang, Chem. Soc. Rev. 39 (2010) 3142–3156.
[8] R.C. Harrison, C.A. McAuliffe, M.E. Friedman, Inorg. Chim. Acta 92 (1984) 43–46.
[9] P. Štarha, J. Marek, Z. Trávníček, Polyhedron 33 (2012) 404–409.
[10] E.J. New, C. Roche, R. Madawala, J.Z. Zhang, T.W. Hambley, J. Inorg. Biochem. 103 (2009) 1120–1125.
[11] J. Pracharova, T. Saltarella, T. Radosova Muchova, S. Scintilla, V. Novohradsky, O. Novakova, F.P. Intini, C. Pacifico, G. Natile, P. Ilik, V. Brabec, J. Kasparkova, J. Med. Chem. 58 (2015) 847–859.
[12] J. Ruiz, V. Rodríguez, C. de Haro, A. Espinosa, J. Pérez, C. Janiak, Dalton Trans. 39 (2010) 3290–3301.
[13] B. Morzyk-Ociepa, K. Dysz, I. Turowska-Tyrk, D. Michalska, J. Mol. Struct. 1103 (2016) 202–211.
[14] F.A. Cotton, T.R. Felthouse, Inorg. Chem. 20 (1981) 584–600.
[15] P. Dufour, Y. Dartiguenave, M. Dartiguenave, N. Dufour, A.M. Lebuis, F. Belanger-Gariepy, A.L. Beauchamp, Can. J. Chem. 68 (1990) 193–201.
[16] F.S. Kong, W.T. Wong, J. Chem. Soc. Dalton Trans. (1997) 1237–1241.
[17] S.B. Zhao, R.Y. Wang, S. Wang, J. Am. Chem. Soc. 129 (2007) 3092–3093.
[18] P. Štarha, Z. Trávníček, J. Vančo, Z. Dvořák, J. Biol. Inorg. Chem. 24 (2019) 257–269.
[19] R.A. Khan, A. de Almeida, K. Al-Farhan, A. Alsalme, A. Casini, M. Ghazzali, J. Reedijk, J. Inorg. Biochem. 165 (2016) 128–135.
[20] B. Rosenberg, L. van Camp, T. Krigas, Nature 205 (1965) 698–699.
[21] T.C. Johnstone, K. Suntharalingam, S.J. Lippard, Chem. Rev. 116 (2016) 3436–3486.
[22] G. Hamilton, U. Olszewski, Expert Opin. Drug Metab. Toxicol. 9 (2013) 1381–1390.
[23] A.M. Krause-Heuer, R. Grunert, S. Kuhne, M. Buczkowska, N.J. Wheate, D.D. Le Pevelen, L.R. Boag, D.M. Fisher, J. Kasparkova, J. Malina, P.J. Bednarski, V. Brabec, J.R. Aldrich-Wright, J. Med. Chem. 52 (2009) 5474–5484.
[24] M. Juchum, M. Günther, E. Döring, A. Sievers-Engler, M. Lämmerhofer, S. Laufer, J. Med. Chem. 60 (2017) 4636–4656.
[25] Y. Zhang, B. Liu, X. Wu, R. Li, X. Ning, Y. Liu, Z. Liu, Z. Ge, R. Li, Y. Yin, Bioorg. Med. Chem. 23 (2015) 4815–4823.
[26] P. Štarha, J. Vančo, Z. Trávníček, Coord. Chem. Rev. 380 (2019) 103–135.
[27] P. Štarha, Z. Trávníček, A. Popa, I. Popa, T. Muchová, V. Brabec, J. Inorg. Biochem. 115 (2012) 57–63.
[28] P. Štarha, J. Hošek, J. Vančo, Z. Dvořák, P. Suchý, I. Popa, G. Pražanová, Z. Trávníček, PLoS One 9 (2014) e90341(11 pages).
[29] P. Štarha, Z. Dvořák, Z. Trávníček, PLoS One 10 (2015) e0136338(17 pages).
[30] T. Muchová, J. Prachařová, P. Štarha, R. Olivová, O. Vrána, B. Benešová, J. Kašpárková, Z. Trávníček, V. Brabec, J. Biol. Inorg. Chem. 18 (2013) 579–589.
[31] J. Pracharova, T. Radosova Muchova, E. Dvorak Tomastikova, F.P. Intini, C. Pacifico, G. Natile, J. Kasparkova, V. Brabec, Dalton Trans. 45 (2016) 13179–13186.
[32] J. Prachařová, F.P. Intini, G. Natile, J. Kasparkova, V. Brabec, Inorg. Chim. Acta 472 (2018) 199–206.
[33] P. Štarha, J. Vančo, Z. Trávníček, J. Hošek, J. Klusáková, Z. Dvořák, PLoS One 11 (2016) e0165062(25 pages).
[34] P. Štarha, Z. Trávníček, I. Popa, Z. Dvořák, Molecules 19 (2014) 10832–10844.
[35] P. Štarha, Z. Trávníček, Z. Dvořák, T. Radošová-Muchová, J. Prachařová, J. Vančo, J. Kašpárková, PLoS One 10 (2015) e0123595(20 pages).
[36] P. Štarha, Z. Trávníček, L. Pazderová, Z. Dvořák, J. Inorg. Biochem. 162 (2016) 109–116.
[37] A. Zamora, V. Rodríguez, N. Cutillas, G.S. Yellol, A. Espinosa, K.G. Samper, M. Capdevila, Ò. Palacios, J. Ruiz, J. Inorg. Biochem. 128 (2013) 48–56.
[38] M.D. Hall, K.A. Telma, K.E. Chang, T.D. Lee, J.P. Madigan, J.R. Lloyd, I.S. Goldlust, J.D. Hoeschele, M.M. Gottesman, Cancer Res. 74 (2014) 3913–3922.
[39] K.G. Samper, V. Rodríguez, E. Ortega-Carrasco, S. Atrian, J.D. Maréchal, N. Cutillas, A. Zamora, C. de Haro, M. Capdevila, J. Ruiz, O. Palacios, Biometals 27 (2014) 1159–1177.
[40] L. Zeng, P. Gupta, Y. Chen, E. Wang, L. Ji, H. Chao, Z.S. Chen, Chem. Soc. Rev. 46 (2017) 5771–5804.
[41] S.M. Meier-Menches, C. Gerner, W. Berger, C.G. Hartinger, B.K. Keppler, Chem. Soc. Rev. 47 (2018) 909–928.
[42] E. Alessio, Eur. J. Inorg. Chem. 2017 (2017) 1549–1560.
[43] R. Trondl, P. Heffeter, C.R. Kowol, M.A. Jakupec, W. Berger, B.K. Keppler, Chem. Sci. 5 (2014) 2925–2932.
[44] C.S. Allardyce, P.J. Dyson, D.J. Ellis, S.L. Heath, Chem. Commun. (2001) (2001) 1396–1397.
[45] C. Scolaro, A. Bergamo, L. Brescacin, R. Delfino, M. Cocchietto, G. Laurenczy, T.J. Geldbach, G. Sava, P.J. Dyson, J. Med. Chem. 48 (2005) 4161–4171.
[46] R.E. Morris, R.E. Aird, P.D. Murdoch, H.M. Chen, J. Cummings, N.D. Hughes, S. Parsons, A. Parkin, G. Boyd, D.I. Jodrell, P.J. Sadler, J. Med. Chem. 44 (2001) 3616–3621.
[47] R.E. Aird, J. Cummings, A.A. Ritchie, M. Muir, R.E. Morris, H. Chen, P.J. Sadler, D.I. Jodrell, Br. J. Cancer 86 (2002) 1652–1657.
[48] A. Bergamo, A. Masi, A.F.A. Peacock, A. Habtemariam, P.J. Sadler, G. Sava, J. Inorg. Biochem. 104 (2010) 79–86.
[49] P. Štarha, Z. Trávníček, J. Vančo, Z. Dvořák, Molecules 23 (2018) 420 (16 pages).
[50] J. Pracharova, V. Novohradsky, H. Kostrhunova, P. Štarha, Z. Trávníček, J. Kasparkova, V. Brabec, Dalton Trans. 47 (2018) 12197–12208.
[51] Y. Arenas, S. Monro, G. Shi, A. Mandel, S. McFarland, L. Lilge, Photodiagn. Photodyn. Ther. 10 (2013) 615–625.
[52] J. Fong, K. Kasimova, Y. Arenas, P. Kaspler, S. Lazic, A. Mandel, L. Lilge, Photochem. Photobiol. Sci. 14 (2015) 2014–2023.
[53] M. Patra, T. Joshi, V. Pierroz, K. Ingram, M. Kaiser, S. Ferrari, B. Spingler, J. Keiser, G. Gasser, Chem. Eur. J. 19 (2013) 14768–14772.
[54] G. Agonigi, T. Riedel, S. Zacchini, E. Paunescu, G. Pampaloni, N. Bartalucci, P.J. Dyson, F. Marchetti, Inorg. Chem. 54 (2015) 6504–6512.
[55] P. Štarha, L. Hanousková, Z. Trávníček, PLoS One 10 (2015) e0143871(19 pages).
[56] J.L. Butour, S. Wimmer, F. Wimmer, P. Castan, Chem. Biol. Interact. 104 (1997) 165–178.
[57] M.N. Alam, F. Huq, Coord. Chem. Rev. 316 (2016) 36–67.
[58] B. Morzyk-Ociepa, K. Szmigiel, I. Turowska-Tyrk, M. Malik-Gajewska, J. Banach, J. Wietrzyk, Polyhedron 153 (2018) 88–98.
[59] K. Dysz, M. Malik-Gajewska, J. Banach, B. Morzyk-Ociepa, J. Mol. Struct. 1181 (2019) 444–454.
[60] C.H. Leung, H.J. Zhong, D.S.H. Chan, D.L. Ma, Coord. Chem. Rev. 257 (2013) 1764–1776.
[61] A. Zamora, G. Vigueras, V. Rodríguez, M.D. Santana, J. Ruiz, Coord. Chem. Rev. 360 (2018) 34–76.
[62] P. Zhang, P.J. Sadler, J. Organomet. Chem. 839 (2017) 5–14.
[63] P. Štarha, Z. Trávníček, H. Crlíková, J. Vančo, J. Kašpárková, Z. Dvořák, Organometallics 37 (2018) 2749–2759.
[64] C.F. Shaw III, Chem. Rev. 99 (1999) 2589–2600.
[65] C. Roder, M.J. Thomson, Drugs R&D 15 (2015) 13–20.
[66] N. Liu, X. Li, H. Huang, C. Zhao, S. Liao, C. Yang, S. Liu, W. Song, X. Lu, X. Lan, X. Chen, S. Yi, L. Xu, L. Jiang, C. Zhao, X. Dong, P. Zhou, S. Li, S. Wang, X. Shi, P.Q. Dou, X. Wang, J. Liu, Oncotarget 5 (2014) 5453–5471.
[67] P. Štarha, Z. Trávníček, B. Drahoš, Z. Dvořák, Int. J. Mol. Sci. 17 (2016) 2084 (16 pages).